The role of BATF2 during of experimental murine Schistosomiasis

by

Thabo Rantanta Victor Mpotje

MPTTHA001

Submitted to the University of Cape Town

In fulfilment of the requirements for the degree

MSc (Med) in Clinical Science & Immunology

Faculty of Health Sciences

University of Cape Town

15th August 2017

Supervisor: Professor Frank Brombacher

Co-supervisor: Dr Justin Komguep Nono

Department of Pathology and Immunology

Declaration

I, *Thabo Rantanta Victor Mpotje*, hereby declare that the work on which this dissertation/thesis is based is my original work (except where acknowledgements indicate otherwise) and that neither the whole work nor any part of it has been, is being, or is to be submitted for another degree in this or any other university.

I empower the university to reproduce for the purpose of research either the whole or any portion of the contents in any manner whatsoever.

Signature: Signed by candidate

signature removed

Date: 15 August 2017

Acknowledgement

I would like to sincerely thank my supervisor, Dr Justin Komguep Nono, for being more than just a supervisor, He became my mentor and showed me rare qualities that a researcher can have. I am grateful for the time he dedicated for me and his students to ensure we are well trained.

I cannot forget about the rest of my team who also sacrificed their time to be there for me and ensure things ran smoothly. I therefore, thank Nada and Lerato for everything they did for me. They were there throughout as my seniors and my sisters. The laughs, advices, and 'Barcelos' that we all shared are part of what got me through. From the bottom of my heart I thank them.

I also thank each and every one in my laboratory for the warmth I have received from working there. I was fortunate enough to work with wonderful and more accommodating people.

I wish to thank my supervisor, Professor Brombacher, for such an opportunity he has offered me and for trusting in my abilities to handle the Master's degree.

I also wish to thank my sponsors, the National Research Foundation (NRF), as well as the Duncan Baxter Scholarship, who made it possible for me to reach this far.

Most importantly I would like to thank family members who have been very supportive and patient with me throughout. First I would like to sincerely thank my 'family' here in Cape Town, the D'Altons who have done for me more than I could have ever asked for. They opened their home to me and made me one of them. I do not know what I would have done without them. For that I am really grateful.

I thank everyone one of my family members in Free State, including all my sisters, my nephews, niece, brothers' in law, and lastly my beautiful mother, Sarah Mofokeng, who has been my pillar through my life's journey.

The thesis is dedicated to my late father, Samuel Mpotje, my late best-friend, Letanta Pintso, and my late girlfriend, Nthabiseng Nthurubele.

Table of contents

Abbreviations:

AP-1	Activator protein 1
APC	Antigen presenting cells
BATF	Basic leucine zipper transcription factor ATF-like
BSA	Bovine serum albumin
bZIP	Basic leucine zipper
cDC	Classical dendritic cells
cDNA	Complementary Deoxyribonucleic acid
EDTA	Ethylenediaminetetraacetic acid
ELISA	Enzyme-linked immunosorbent Assay
ES	Embryonic stem cell
FACS	Fluorescent Activated Cell Sorting
FCS	Fetal calf serum
FcγRIII	Fc gamma receptor 3
Frt	Flippase recognition target
H&E	Haemotoxylin and eosin
iFBS	Inactivated Foetal Bovine Serum
IFN- γ	Interferon gamma
IL-	Interleukin-
IMDM	Iscove's Modified Dulbecco's Medium
IRF	Interferon-regulatory factor
LoxP	Locus of X-over in P1
M1	Classically activated macrophages
M2	Alternatively activated macrophage
MgCl	Magnesium chloride
MLN	Mesenteric lymph node
Neo	Neomycin
PBS	Phosphate buffered saline
Pen-strep	Penicillin-Streptomycin
PMA	Phorbol 12-myristate 13-acetate

pmol	picomolar
PNP	P-Nitrophenyl phosphate
qPCR	Quantitative Polymerase chain reaction
RBC	Reb blood cell
RNA	Ribonucleic acid
RPE buffer	RNA precipitation elution buffer
Rpm	Revolutions per minute
S. mansoni	*Schistosoma mansoni*
SANS	South African National Standard
SD	Standard deviation
SEA	Soluble egg antigen
STAT 2	Signal transducer and activator of transcription 2
TBE	Tris/Borate/EDTA
Tfh	Follicular helper T cell
TGF-β	Tumour growth factor beta
Th	T helper
TNF-α	Tumour necrosis factor alpha
WHO	World Health Organization
WT	Wild type

List of figures.

Abstract:

Schistosomiasis is one of the most debilitating tropical diseases with the potential to cause morbidity and mortality in infected populations unless well controlled. Current control measures are limited to treatment with praziquantel. A rather alarming situation given i) the inability of the drug to directly target the pathogenic eggs, ii) the emergence of praziquantel-resistant schistosomes, iii) the persistence of tissue fibro-proliferative destruction caused by the trapped parasite eggs, even after treatment. Intestinal and liver immunopathology are pathognomonic of schistosomiasis and generally result from the host inadequate Th2 and or Th17 responses to the egg-derived antigens. Failure to control these immune responses causes the most of the detriment to the infected host, highlighting the need for a better understanding of the regulatory mechanisms which might help prevent excessive immune responsiveness and the ensuing immunopathology.

A Basic leucine zipper transcription factor ATF-like 2 (BATF2) which belongs to a family of transcription factors critical in the control of inflammatory responses has gained enormous momentum recently as a potential target to immune deregulation during cancer and infectious diseases. We reasoned that an eventual BATF2 influence on the host immune response during schistosomiasis might unveil its anti-disease potency and greatly facilitate the quest for a novel control strategy against the immunopathology during schistosomiasis. Addressing this in our present study, BATF2-deficient mice were used and characterized for immunological and physiological parameters during steady state and Schistosomiasis. Although the liver showed a reduced pro-fibrotic response, there was a notable increase of several pro-fibrotic cytokines (TNF-α, IFN-γ, TGF-β and IL-13) Which further translated into an elevated level of granulomatous inflammation and fibrosis in the gut of *S. mansoni* infected BATF-2-deficient mice when compared to the liver tissues of BATF2-deficient mice and both livers and intestines of infected littermate controls indicating that BATF2 appears to have a tissue-specific role on the regulation of fibrogranulomatous inflammation during schistosomiasis. Therefore, BATF2 has a critical, and hitherto unappreciated, role in mediating the regulation of gut fibrogranulomatous response so as to promote host survival during schistosomiasis.

1. Literature review:

1.1. Schistosomiasis

1.1.1. Schistosomiasis disease and the disease-causing agents/species

Schistosomiasis also known as bilharzia or snail fever, is a prevalent disease that is caused by parasitic worms of the genus *Schistosoma* (Pedras, 1996) resulting in acute and chronic disease mainly carried by fresh water snails (Sabin Vaccine Institute, 2015; WHO, 2017). The species of the genus include *Schistosoma mansoni* (*S. mansoni*), *Schistosoma japonicum* and *Schistosoma haematobium* (*S. haematobium*) being the major causes of human morbidity and mortality (Pearce, 2002; Cavalcanti, 2015). The disease predominantly affects tropical and sub-tropical regions with the majority of people affected by the disease being in Africa (Sabin Vaccine Institute, 2015). Moreover, the infection rate of the disease is higher in children than in adults since they are more in contact with contaminated freshwater (Gryseels, 2016; WHO, 2017). Schistosomiasis is regarded as a disease of poverty and one of the most common parasitic diseases ranking second only to malaria (Sabin Vaccine Institute, 2015; WHO, 2016). *S. mansoni* is the most widespread of human-infecting schistosomes developing a spectrum of symptoms, together with *S. japonicum*, which includes cercarial dermatitis and tissue inflammation within the liver and intestines of infected individuals, as well as severe hepatosplenic schistosomiasis (Hams, 2013).

1.1.2. Life cycle of *S. mansoni*

The lifecycle of the *S. mansoni* as shown in figure 1 (Dunne, 2005), involves two main hosts including humans and snails of the species *biomphalaria glabrata*. The parasite eggs that are released into fresh water hatch upon optimal conditions and release the miracidia which then swim around seeking a specific

snail intermediate host to infect. The miracidiae, once in a snail intermediate host, multiply and generate sporocysts which develop into larvae called cercariae (Centers for Disease Control and Prevention, 2012). The cercariae are released from the snails into fresh water ready to infect a human host. When they come into contact with a human, they attach and crawl along the skin looking for entry points such as sweat glands where they penetrate the skin - initiating an infection (Haas and Schmitt, 1982). The cercariae will shed their forked tail transforming into schistosomulae which will enter the vasculature and migrate to the mesenteric veins, where they mature into adult worms (Pearce, 2002; Wilson, 2007; Centers for Disease Control and Prevention, 2012). The adult parasites can live up to 10 years or more in the mesenteric veins, releasing hundreds of eggs each day (Pearce, 2002). Some of the eggs are released back into the environment via faeces, while others get trapped in the microvasculature of the liver and the gut. At this point the eggs induce a vigorous granulomatous response that is characterized by the development of fibrosis and portal hypertension which are the primary causes of morbidity and mortality in infected individuals (Pearce, 2002).

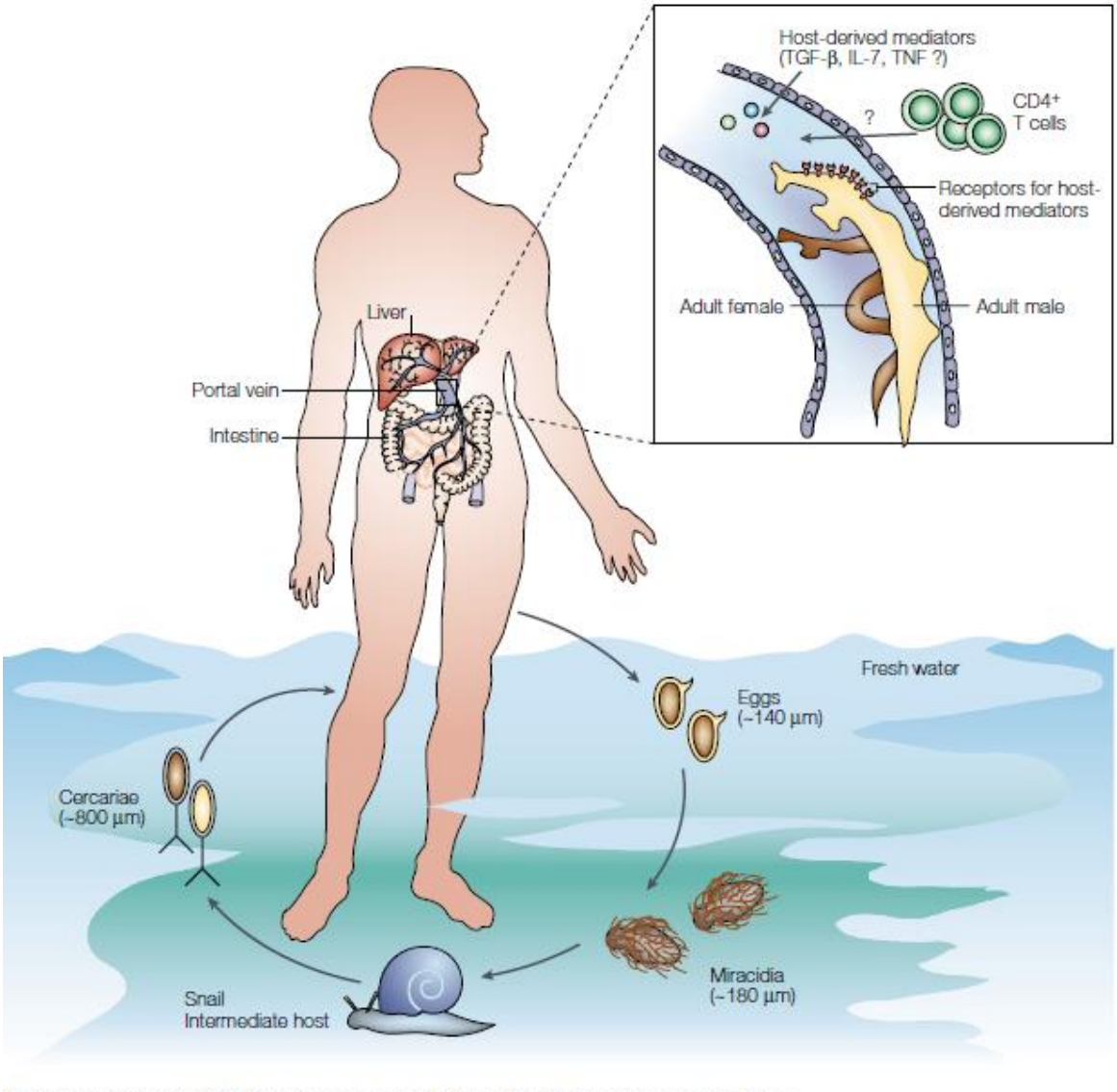

Figure 1: Life cycle of *Schistosoma mansoni* (Dunne, 2005)

1.1.3. **Epidemiology (transmission and control of disease) of *S. mansoni***

Schistosomiasis is mostly prevalent in tropical and sub-tropical regions, and affects mainly poor communities, especially agricultural and fishing populations, who do not have access to safe drinking water or adequate sanitation (WHO, 2017). People, mostly from endemic areas, get infected with the parasites during routine agricultural, domestic, occupational, and recreational activities which provides the basis for exposure to contaminated water (WHO, 2017). Among the population of individuals exposed to the parasites, school children are more at

risk and show a high infection rate due to lack of hygiene and certain play habits which include swimming and or wading (Centers for Disease Control and Prevention, 2012; Gryseels, 2016; WHO, 2017). Women are also at high risk of infection from exposure to infested water given their domestic chores which include doing laundry in rivers. Tourist attraction sites/areas such the Nile valley in Sudan and Egypt also serve as high risk areas of infection by the parasites, especially the *S. mansoni* species (Centers for Disease Control and Prevention, 2012). The *S. mansoni* are mainly distributed throughout Africa, South America (Brazil, Suriname, and Venezuela). The Caribbean islands of Dominican Republic, Guadeloupe, Martinique, and Saint Lucia have low infection rates. The increased risk of infection is mainly around areas of freshwaters such as lakes, rivers and small bodies of water (Centers for Disease Control and Prevention, 2012; WHO, 2017). The disease reaches urban areas due to population movements which include tourists, facility transmission, and the need for water sources (WHO, 2017).

1.1.4. **Diagnosis of Schistosomiasis**

The disease is mainly diagnosed through parasitological techniques that detects for the presence of parasite eggs in stool (*S. mansoni*) or urine (*S. haematobium*) specimens (van Dam, 2004; WHO, 2017). Although such techniques have limitations in that they include a high fluctuation in egg counts, one could easily misdiagnose low infections, and these techniques are usually time consuming (van Dam, 2004). The immunological techniques are also employed to diagnose the disease by detecting antigens, or antibodies raised against the parasite antigens in blood or urine (van Dam, 2004; WHO, 2017). These techniques have higher sensitivity of detection, although they require more advanced laboratory settings.

1.1.5. **Disease complications and current estimates of burden**

Individuals infected with schistosomes develop a plethora of symptoms that can clustered depending on the species. The essential of symptoms associated with all schistosomiases is provided by a seminal review article of Ross and Collaborators (Ross *et al*., 2002). For the purpose of the present work, however, the emphasis is on the clinical features of infections caused by *S. mansoni*. Individuals affected by *S. mansoni* often develop a spectrum of symptoms which include cercarial dermatitis and tissue inflammation within the liver, and intestines. These can lead to a more severe hepatosplenic schistosomiasis (Hams, 2013). Previous studies have shown that the pathology observed during schistosomiasis is a result of an excessive or dysregulated inflammatory response to the parasite eggs that become trapped in various tissues (primarily liver and gut) of the infected individual (Hams, 2013). Schistosomiasis is characterized by two main clinical conditions termed acute schistosomiasis and chronic schistosomiasis (Pearce, 2002) which are mediated by different immune responses, as primarily gleaned from experimental murine studies and confirmed in human trials (Romagnani, 1992). Acute schistosomiasis mainly develops in individuals who are non-immune travellers with symptoms, such as fever, cough, muscle aches, and rash, appearing 2 to 12 weeks post exposure (Leshem, 2008; Centers for Disease Control and Prevention, 2012). In the case of chronic schistosomiasis, affected individuals display clinical symptoms such as abdominal pain, bloody diarrhoea or hematuria, anemia, splenomegaly and hepatomegaly (Centers for Disease Control and Prevention, 2012). In severe cases, the parasite eggs could pass through the blood brain barrier and cause seizures, paralysis, and or spinal cord inflammation (Centers for Disease Control and Prevention, 2012). With these alarming clinical conditions in infected individuals, it is estimated that more than 800 million individuals are at risk of infection from schistosomiasis globally, of which approximately 250 million are already infected (Sokolow, 2016; Loke *et al*., 2002; Caffrey, 2007; Chitsulo *et al*., 2000; Hotez *et al.*, 2006). The infection results in an estimated 280 000 deaths per year in endemic areas such Sub-Saharan Africa (van der Werf *et al.*, 2003).

1.1.6. **Schistosomiasis treatment and current control measures**

Treatment of the disease is mainly carried out with praziquantel which is reported to have a success cure rate of 65% to 90 % after a single treatment. Corticosteroids are also used as adjunct therapeutics in debilitating cases (Ahmed, 2017) However, the praziquantel does not protect against re-infection and besides the known anti-parasitic effect on adult schistosome worms, this reference drug is ineffective against developing schistosomula and does not directly target the pathogenic eggs (Olds, 2003). The drug might also become ineffective as recent reports have now surfaced to suggest that clinical schistosomes isolated in some hyperendemic area are becoming more resistant to Praziquantel (Vale, 2017; Melman, 2009; Ishmail, 1999).

1.2. **Immune polarization and the control of schistosomiasis pathology**

1.2.1. **Immune cell development and selection**

Dendritic cells play an essential role linking innate and adaptive immune responses during infections or encounter with antigens allowing naïve T cells to differentiate into antigen specific effector T cells (Oh, 2015; Banchereau, 1998). When the dendritic cells recognise an antigen through pattern recognition receptor (PRR) they initiate phagocytosis leading to processing and loading of the processed antigen on major histocompatibility complex presented on the surface of the cells (Hossain, 2013; Medzhitov, 2007). The MHC-peptide complex is further recognised in thymus by naïve T cells which express T cell receptor (TCR) allowing differentiation into a protective CD4+ or CD8+ T cell response against the antigen presented by MCHI or MCHII respectively (Oh, 2015). Selection of T cells in the thymus is dependent on both foreign and self-antigens which helps mediate adequate immune responses that either clears off the foreign antigens via effector T cells, or tolerates via regulatory T cells, the self-antigens to prevent the development of harmful autoimmunity (Oh, 2015).

In some cases tolerogenic/suppressive immune response is also mounted toward foreign antigens (Oh, 2015), and this is mainly in tissues such the intestine which is constantly exposed to food and commensal antigens (Oh, 2015; Tomasello, 2013). The immune response in the intestine has developed a complex system that allows discrimination of commensal microbes and pathogens which could trigger complications such as inflammatory bowel or coeliac disease (British Society for Immunology, 2017). The intestinal immune system is comprised of intestinal epithelial lymphocytes (IEL), intra epithelial lymphocytes (ILF), and tissue-specific organised lymphoid structures (Peyer's patches, mesenteric lymph nodes, cryptopatches and isolated lymphoid follicles) which all work together to help the intestinal tissue to take up nutrients and fluids while discriminating against pathogenic antigens (Tomasello, 2013)

1.2.2. **Host response during the initial phase of infection**

During early stage of infection (3 – 5 weeks), migrating immature parasites drive a dominant type 1 immune response as judged by the expansion of T helper (Th) 1 cells, classically activated macrophages (M1) and the release of cytokines such as Tumour necrosis factor (TNF), interferon gamma (IFN-γ) (de Jesus, 2002; Wynn, 1993; Bogen, 1995).

1.2.3. **Host response during the acute phase of infection**

As the parasite development continues and results in the production of eggs by female adults, a type 2 dominated acute response is mounted between 6 to 10 weeks post infection (Bogen, 1995; Fallon, 2007; Wilson, 2007). The acute response is characterized by type 2 granulomatous inflammation which results from the accumulation of $CD4^+$ T helper 2 cells, eosinophils, and alternatively activated macrophage (M2) around the eggs lodged in tissues, and the release of type 2 effector cytokines such as IL-4, IL-5, and IL-13 (Fallon, 2007; Pearce, 2002; Boros, 1999). In the event of *S. mansoni* products (eggs) being released,

antigen presenting cells (APC) such as dendritic cells interact with the antigens, process and present them to $CD4^+$ T cells which will initiate a protective type 2 inflammatory response (Rutitzky, 2007; Pearce, 2002; Hammerich, 2010). In most cases the CD11b+ dendritic cells initiate the activation of a more protective $CD4^+$ T cell response during *s. mansoni* infection, that is polarized into a Th2 phenotype, characterised by the production of IL-4, IL-5, and IL-13, and is driven by signal transducer and activation of transcription factor (STAT) 6, GATA-3 and IL-4 (Rutitzky, 2007; Hammerich, 2010; Mayer, 2017). In the event of this protective Th2 response, a type 1 $CD8^+$ T cell response is also concurrently initiated to regulate the development of exacerbated Th2 response (Pedras-Vasconcelos, 1996), and this response was recently shown to be driven by BATF3-driven $CD8^+$ dendritic cells through constitutive expression of IL-12 (Everts, 2015).

However, in severe cases of schistosomiasis, the CD4+ T cells are more polarized into a pathogenic Th17 phenotype that is driven by TGF-β and IL-23 and is characterized by expression of orphan nuclear receptor RORγt as well as production of IL-17 (Rutitzky, 2007; Hammerich, 2010). It has previously been suggested that the mechanism in which the Th17 cells cause a severe pathology in the case of Schistosomiasis is through the recruitment of granulocytes such as eosinophils (Rutitzky, 2007). It is therefore, imperative that both type 1 and type 2 immune responses are co-actively initiated to mount an equilibrated, protective and well controlled immune response with no or less pathological consequences during acute Schistosomiasis. To achieve this, a more detailed understanding of the mechanisms and factors contributing to a well-controlled protective immune response, is required during acute schistosomiasis.

1.2.4. **Host response during the chronic phase of infection**

Following the acute phase is a more regulatory response starting as from week 10 post-infection onwards (Fallon, 2007; Pearce. 2002). In this phase, the type-2 inflammatory response against the trapped parasite eggs is mitigated and the rapidly expanding regulatory response aids the establishment of chronicity

(Schmiedel, 2015; Pearce, 2002). Additionally, an intrinsic Th2 cell hypo-responsiveness is also suggested to contribute to the establishment of chronicity during schistosomiasis (Yang, 2009; Wilson, 2007) further illustrating the rather complex nature of the regulatory processes that dictate the establishment of a minimally pathogenic chronic phase during schistosomiasis (Pearce, 2002; Vasconcelos, 1996).

1.2.5. **Current evidences of the therapeutic value of altering immune polarization during schistosomiasis.**

Two major immune defects account for the majority of the morbidities associated with schistosomiasis. These are: i) the host inability to mount an appropriate inflammatory response to entrap within a robust granuloma the released toxins from the parasite eggs and ii) the host inadequate regulatory response to tame the fierce anti-egg response elicited during acute schistosomiasis as the infection progresses towards equilibrium (Ramadan, 2013; Wang, 2015). These failures usually result in heightened tissue pathology and eventually premature death as extensively reported in murine models (Herbert, 2004; Leeto, 2006). With no vaccine and a rather limited, albeit still efficacious praziquantel-based chemotherapy available, an accumulating number of reports have now successfully addressed the possibility of ameliorating tissue pathology thus morbidity by altering the host immune response during experimental schistosomiasis (Ramalingam, 2016). In these studies, a striking ability to reduce excessive tissue fibrosis thus schistosomiasis-driven pathology was achieved by either blocking IL-13 alone (Mentink-Kane, 2004), dually blocking IL-13 and IFN-g (Chiaramonte, 2003) or completely interrupting IL-13 and IL-4 signalling via Interleukin-4 receptor alpha (Nono *et al*., In press).

1.3. A host factor regulating immune polarization: the basic leucine zipper ATF-like (BATF)-2 transcription factor

1.3.1. Definition of the BATF family of transcription factors

Basic leucine zipper transcription factor ATF-like (BATF) 2 belongs to a family of transcription factors called BATF family which in turn belongs to a family of transcription factors called activator protein 1 (AP-1) (Murphy, 2013). The BATF family comprises of BATF, BATF2, and BATF3, which play a role in the development and regulation of the immune cells.

1.3.2. Role of BATF family members in immunity

BATF and BATF3 have been shown to be involved in the development and regulation of B cells, dendritic cells, T cells, and macrophages (Murphy, 2013). The transcription factors are characterized by α-helical basic leucine zipper (bZIP) structures. The structures contain a basic DNA binding region and a leucine zipper domain which allows members of this family to form heterodimers with other AP-1 family members such as JUN proteins and non AP-1 members including interferon-regulatory factor 1 (IRF1), IRF4, and IRF8 (Murphy, 2013).

i) BATF is one of the extensively studied transcription factors that is mainly involved in development and regulation of immune cells such as Th9, Th17, follicular helper T (Tfh) cell, adipose tissue-resident regulatory T cells and effector CD8+ T cells (Guler, 2013). The transcription factor also regulates the immunoglobulin class switching in B cells as well as the expression of GATA3 and effector factors (IL-4, IL-10, CTLA4) in Th2 cells (Betz, 2010; Ise, 2011). Studies have demonstrated the transcription factor as a central modulator of peripheral and humoral hallmarks of type 2 immune response during anthelminthic immunity which helps in establishment of an adequate type 2 immunity during infection (Bao, 2016).

Ii) On the other hand, BATF3 is reported to be involved in the development of CD8α + dendritic cells and both BATF and BATF2 can compensate for its function (Hildner, 2008).

iii) BATF2, unlike the other members of BATF family, is being increasingly studied only of recent. Besides its initial role elegantly defined in the compensation for BATF3 deficiency during the development of CD8α + dendritic cells (Hildner, 2008), evidences have now been provided for the massive induction of BATF2 in type-1 polarized macrophages to sustain inflammatory responses *in vitro* during mycobacterial infection (Roy, 2015). Furthermore BATF2 was also shown to suppress Th17-driven responsesthrough the suppression of IL-23 production by dendritic cells during experimental trypanosomiasis (Kitada, 2017).

1.3.3. **Role of BATF family during disease**

The BATF family members are shown to play crucial roles in coordinating the immune system activities which are critical in autoimmunity, inflammation and the host response to pathogens (Muphy, 2013; Roy, 2015, Hildner, 2008) with the BATF being identified as a central modulator of peripheral and humoral hallmarks of type-2 immunity during anthelminthic immunity (Bao, 2016). The BATF3 on the other hand was reported to drive Th1 immunity through the production of IL-12 to protect against Leishmania major or to suppress helminth-driven type-2 immunity (Mart´ınez-L´opez, 2015; Everts, 2015).

The BATF2 was first assigned a role in the development of CD8+ dendritic cells, and was later shown to also induce type-1 inflammatory responses in classically activated macrophages during mycobacterium tuberculosis infection (Roy, 2015). A recent study by Kitada *et al.*, has reported on the role of BATF2 to inhibit immuno-pathological Th17 response during *Trypanosoma cruzi*, through the suppression of production of IL-23 (Kitada *et al.*, 2017).

Therefore, BATF family members in general, and BATF2 in particular, appear to be considerably relevant for the coordination and regulation of inflammatory responses during disease and as such, attractive targets for the immune-alteration of immunopathological processes they might govern in disease, a strategy that has already gathered a heavy momentum in the context of cancer research (Guler, 2015).

1.4. **Problem statement and justification of the present project**

BATF2, a now increasingly reported host inflammatory regulator in cancer and infectious diseases (Roy, 2015; Guler, 2015; Ma, 2011) is still poorly studied in the context of helminth infections. The present study, therefore attempted to explore further the role of this transcription factor during Schistosomiasis and provide a better understanding on how the targeting of this factor could be exploited to improve the current disease control measures given its potential to regulate helminth driven pathology.

1.5. Hypothesis

Given the reported role of BATF2 in the induction of Th1 and suppression of Th17 responses during infections, we hypothesized that BATF2 deficiency may promote Th2 and Th17 responses during acute schistosomiasis and result in morbidity and possibly mortality in *S. mansoni*-infected mice.

1.5. **Aim and objectives of the study**

1.6.1 The aim of the study was to assess the role of BATF2 during experimental Schistosomiasis.

1.6.2. Objectives

To achieve our aim, we set forth

- To measure the changes in expression rates of BATF2 in the liver and intestinal tissues of mice following *S. mansoni* infection.
- To characterize a BATF2 deficient mouse model.
- To characterize the immune and pathological responses that associate with the absence of BATF2 during acute infection with *Schistosoma mansoni.*
- To determine the survival rate of BATF2 deficient mice during infection with *Schistosoma mansoni*.

2. Materials and methods

2.1. Ethics statement

All the experiments performed were conducted in accordance with the Animal Research Ethics Committee of South African National Standard (SANS 10386:2008) and University of Cape Town, South Africa for practice on animal procedures. The study protocols (Permit numbers: 014/003 and 016/027) were approved by the Animal Ethics Committee, Faculty of Health Sciences, University of Cape Town (Cape Town, South Africa).

2.2. Generation, genotyping and characterization of BATF2 deficient mice

BATF2 deficient mice were generated from the 129 background mice which demonstrate a skewing of the immune response towards a more Th2 responses ideal for studying helminth infections, than the C57BL/6 which demonstrate skewing towards Th1 responses (O'Neill *et. al*., 2000). The 129 mice are generally poor learners and thus cannot be utilized for behavioural studies (Rivera *et. al.*, 2008), but unlike with the C57BL/6 mice, the 129 are not limited to certain immunological questions such as the development of tumor unlike the C57BL/6 mice which are resistant to tumor development (O'Neill *et. al*., 2000).

Wild type (WT) and BATF2$^{-/-}$ 129SvEv mice were generated using homologous recombination (figure 2) and purchased from The Jackson Laboratory. Briefly: A targeting vector was initially designed with a gene containing a loxP site, an frt site, a neomycin resistance (neo) cassette in reverse orientation, a second loxP and frt sites. The gene was used, from 5' to 3', to replace exons 1-2 of the basic leucine zipper transcription factor, ATF-like 2 (BATF2). The new recombinant construct was then electroporated into 129S6/SvEvTac-derived EDJ22 embryonic stem (ES) cells. ES cells with the new gene construct were then injected into blastocysts resulting in chimeric mice. The male chimeric mice were bred to 129S6/SvEv females resulting in some of the mice being 129S6/SvEvTac

which were later inbred for at least one generation to establish the colony. All mice are housed under quarantine conditions in the University of Cape Town animal facility. Figure 2. Generation of a targeting construct for BATF2 mice by homologous recombination.

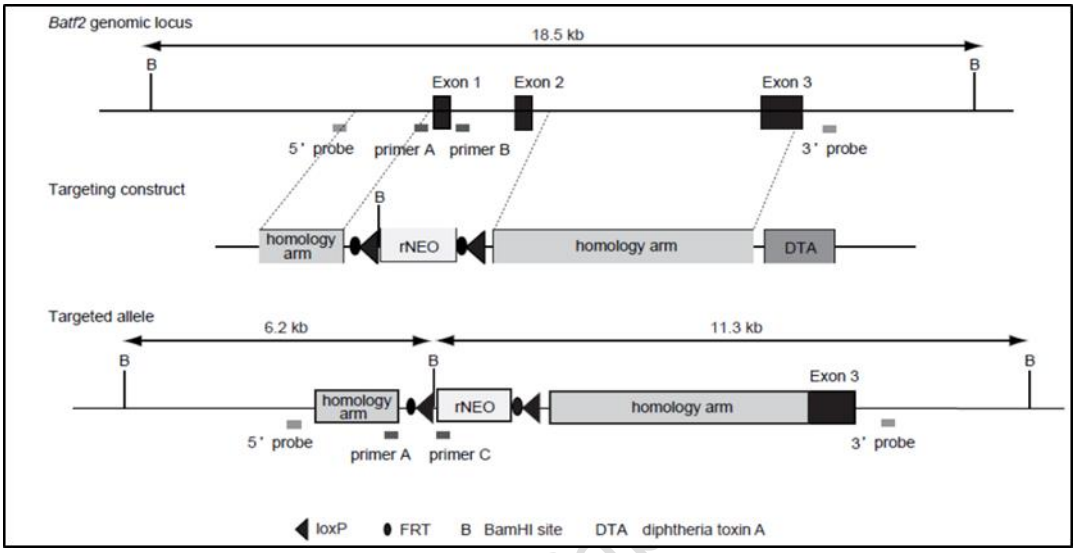

Figure 2: Generation of a targeting construct for BATF2 mice by homologous recombination.

Mice were genotyped using PCR to determine whether the BATF2 exons 1 and 2 were removed from the genome of BATF2$^{-/-}$ mice using the following primers: Forward primer 5' 3', and reverse primer BATF2 P1 (5'-ACC CTC CAC CAT CCT TCT TC), BATF2 P2 (5'- GAC TGG TCT GCA GTG TGA GC), BATF2 P3 (5'-CCA GCT CAT TCC TCC CAC T)..

2.3. **Maintenance of *S. mansoni* life cycle**

Biomphalaria glabrata snails together with BALB/c female mice were used to expand and maintain the *S. mansoni* parasites which were maintained and monitored in Bio-Safety level 2, University of Cape Town.

2.4. Experimental murine infection with *S. mansoni*

2.4.1. Acute infection: Identifying the role of BATF2 during acute infection of *S. mansoni*.

A total of 32 mice were used for the experiment. Sixteen wild type ($BATF2^{+/+}$) and 16 ($BATF2^{-/-}$) knockout mice, both female and male ranging between 7 - 12 weeks old, were percutaneously infected with 100 live cercariae of *S. mansoni* obtained from the *Biomphalaria glabrata* snails. The mice were monitored 1-2 times a day, weighed weekly and recorded for a period of 7 weeks. Approximately 500 – 600 µl of blood was collected using cardiac puncture, and organ weights which include liver, spleen, heart, and lung were measured recorded and collected. Abdomens of euthanized mice were exposed to observe and capture any physiological damages that could possibly result in experimental end-point of the mice.

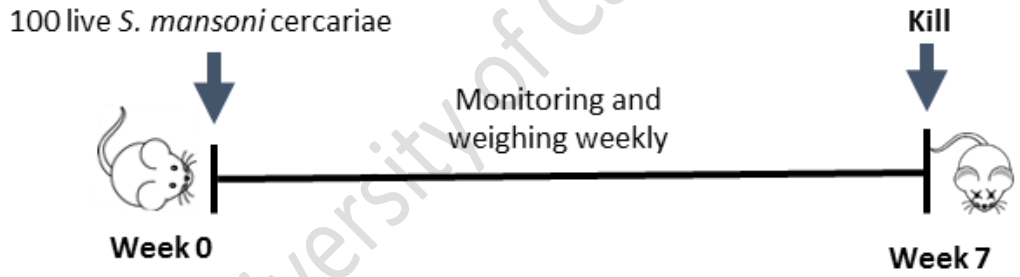

Figure 3: Acute infection protocol to be followed

2.4.2. Mortality infection: Survival rate of BATF2 deficient mice post *S. mansoni* infection.

A total of 36 mice were used for the experiment. Eighteen wild type ($BATF2^{+/+}$) and 18 ($BATF2^{-/-}$) mice, both female and male ranging between 6 - 8 weeks old, were percutaneously infected with 80 live cercariae of *S. mansoni* obtained from the *Biomphalaria glabrata* snails. The mice were monitored for mortality 1-2 times a day, weighed weekly and recorded until they reached experimental endpoint.

The experimental end point of the mice infected with *S. mansoni* parasites were reached when each mouse showed the following symptoms: Loss of weight up to 20% from its original body weight, highly reduced activity indicating discomfort, uneven and sticking out of fur, inability to open eyes wide, and loss of strength as evidenced from inability to grip on a metal bar cage.

Final body weight was recorded and approximately 500 – 600 µl of blood was collected using cardiac puncture. Abdomen of euthanized mice were exposed to observe and capture any physiological damages that could possibly result in experimental end-point of the mice.

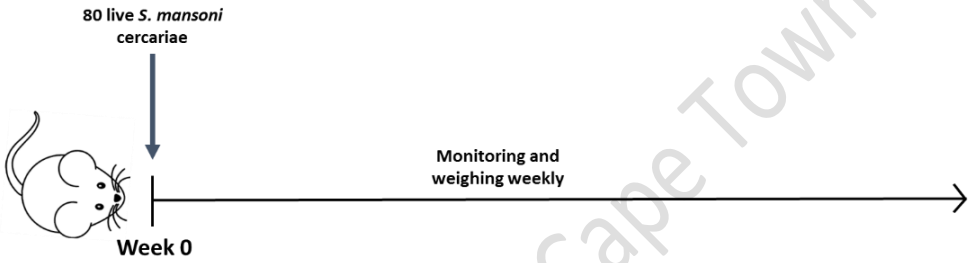

Figure 4: Mortality protocol to be followed.

2.5. Assessing BATF2 gene expression levels in tissues

2.5.1. RNA extraction

RNA was extracted by first homogenizing tissue samples and then used RNA elute Column protocol (Qiagen, USA) to carry out the extraction. The samples were vigorously mixed using a vortex for 1 minute and 200 µl of chloroform was added in each sample containing 1ml of Qiazol. The samples were mixed vigorously by shaking up and down then incubated for 3 minutes at room temperature. Again the samples were vigorously shook and then centrifuged for 15 minutes at 10 000 revolutions per minute (rpm) in a 4^0C microfuge. The colourless upper aqueous layer was then transferred into a new tube and 1ml of 70% ethanol was added to the lysate and mixed by pipetting. Seven microliters of the sample, including the precipitate that formed, to an RNeasy spin column

placed in 2ml collection tube. The samples were then centrifuged for 15 seconds at 10 000 rpm and the flow-through was discarded. Seven hundred microliters of RW1 buffer was added to the RNeasy spin column centrifuged for 15 seconds at 10 000 rpm. The flow through was discarded removing all residues of the flow-through and 500µl of RPE buffer was added to the RNeasy spin column then centrifuged for 15 seconds at 10 000 rpm. Another 500µl of RPE buffer was added was added to the spin column and centrifuged for 2 minutes at 10 000 rpm. The RNeasy spin column was then transferred into a new 2ml collection tube and centrifuged for the tubes for 1 minute at full speed. The RNeasy spin column was transferred again, into a new 1.5ml collection tube and then centrifuged for 1 minute at 10 000 rpm with the flow-through containing RNA samples needed for further analysis. The presence of RNA was confirmed by measuring of samples using a nanodrop ND1000 (Thermo Scientific, USA) and by loading a preheated mixture of 15µl of sample and 1µl of 1x loading buffer in a 1.5% agarose gel composed of 1.5g of agarose powder in 100ml of 0.5X TBE buffer and heated for 5 minutes, plus 10µl of Sybr safe DNA stain (Thermo Scientific, USA). The gel was allowed to run for 40 minutes using 150V of voltage.

2.5.2. **cDNA synthesis**

The cDNA Synthesis was carried out to reverse transcribe the extracted unstable RNA into a more stable cDNA molecule. An amount of 10µl of each sample was added into correctly labelled sterile, nuclease-free thin-walled PCR tubes. One microliters of Anchored-oligo (dT) 18 primer (50 pmol/µl) plus 2µl of Random hexamor primer (600pmol/µl) were added to the samples and mixed them. The template-primer mixture was then denatured by heating the tubes for 10 minutes at 65^0C in a thermal block cycler (BioRad PTC-100, USA). The tubes were immediately cooled on ice. A first strand synthesis cocktail composed of 1X Transcriptor Reverse Transcriptase reaction buffer (8mM $MgCl_2$), plus 20 units of protector RNase Inhibitor (40U/µl), plus 1mM of each of the deoxy-nucleotides, and 10 units of transcriptor reverse transcriptase, was added to the tubes containing the RNA samples and mixed gently. The tubes were then placed in the thermal block with a heated lid and the incubated the reactions using the following conditions: 10 minutes at 25^0C, 60 minutes at 50^0C, 5 minutes at 80^0C,

and the PCR reaction was then stopped by placing the tubes on ice for 5 minutes and then stored in -80^{0}C freezer until further analysis.

2.5.3. **Quantitative Polymerase Chain Reaction (qPCR)**

Quantitative polymerase chain reaction was carried out on the cDNA samples obtained above to measure levels of target gene expression in liver and gut tissues.

2.6. **Single Cell preparations**

2.6.1. **Single cell preparations from Mesenteric Lymph Nodes and Thymus**

Mesenteric Lymph Nodes and Thymus were collected in 2ml Eppendorf tubes containing 1ml of Iscove's Modified Dulbecco's Medium (IMDM) (Gibco, USA) supplemented with 10% heat inactivated Fetal Bovine Serum (iFBS) (Roche Diagnostics, Germany) and 0.5% Penicillin-Streptomycin (Pen-strep) (Gibco, USA). Each sample was teased through a 70µm sieve (Thermo Scientific, USA) on a petri-dish. The solution was further collected and sieved through 40µm sieve into a new labelled 50µl tube, and then topped up to 5ml total solution. The samples were centrifuged for 10 minutes at 1200 rpm and the supernatant was discarded, then re-suspended the samples in 5ml medium (IMDM supplemented with 10% iFBS and 0.5% Pen-strep). The cells were then counted using 2% trypan blue using 1 in 20 dilution.

2.7. **Single cell preparations from Liver and gut**

Liver samples were collected in 15ml tubes containing ice cold 5ml medium (IMDM supplemented with 10% iFBS and 0.5% Pen-strep. The samples were placed on a petri-dish and chopped into small pieces then placed into 15ml tube containing 5ml digestion buffer (IMDM supplemented with 5% iFBS, plus 50 U/ml Collagenase I or II (Sigma, USA), plus 13µg/ml DNase (Thermo Scientific, USA). The samples were then placed inside a 37^{0}C incubator with a shaker for 30

minutes. After the incubation, they were sieved through a 100µm sieve on a petri-dish and sieved again through a 70µm sieve into a new 50ml tube. The samples were centrifuged for 10 minutes at 1200 rpm in a 4^0C and then discarded the supernatant. Three millilitre of PBS + 3% foetal calf serum (FCS) was used to re-suspend the samples and then added 1.7ml of isotonic percoll (9ml percoll + 1ml of 10X PBS), and then mixed thoroughly by inverting the tubes gently. The tubes were centrifuged for 10 minutes at 500g in 4^0C without brakes. The supernatant was carefully removed from the tubes and 5ml of red blood cell (RBC) lysis buffer was used to re-suspend the samples, then incubated for 10 minutes at room temperature. Five millilitre of medium (IMDM supplemented with 10% iFBS and 0.5% Pen-strep) was added to the solutions and then centrifuged for 10 minutes at 1200 rpm in 4^0C. The supernatant was carefully removed and the samples were re-suspended in 1ml of medium (IMDM supplemented with 10% iFBS and 0.5% Pen-strep). The cells were counted using 2% trypan blue using 1 in 2 dilution.

2.8. **Single cell preparations from Spleen**

Spleen samples were collected in 2ml Eppendorf tubes containing 1ml of medium (IMDM supplemented with 10% iFBS and 0.5% Pen-strep). Each sample was teased through a 100µm sieve (Thermo Scientific, USA) on a petri-dish and was further sieved through a 70µm sieve into a new 50ml tube. The samples were centrifuged for 10 minutes at 1200 rpm and the supernatant was discarded then re-suspended the samples in a 5ml red blood cell (RBC) lysis buffer (8.24g Ammonium chloride (NH_4Cl) + 0.037g EDTA + 1g $NaHCO_3$ + 1 litre of 1X PBS) and incubated for 10 minutes at room temperature. After the incubation, 3ml of medium was added and the samples were centrifuged for 10 minutes at 1200 rpm again. The supernatant was discarded then re-suspended the samples with 5ml medium and sieved through a 40µm sieve into a new 50ml tube and centrifuged for 10 minutes at 1200 rpm. The cells were counted using 2% trypan blue using 1 in 10 dilution.

2.9. **Single cell preparations from Lung**

Spleen samples were first placed on a petri-dish and chopped into small pieces and collected in a 15ml tubes containing 5ml of digestion medium (IMDM supplemented with 5% iFBS, plus 50 U/ml Collagenase I (Gibco), plus 13µg/ml DNase I. The samples were incubated for 30 minutes at 37^0C. After the incubation, the samples were teased through a 100µm sieve on a petri-dish. The samples were further sieved through a 70µm sieve into a new 50ml tube and then centrifuged for 10 minutes at 1200 rpm. The cells were then re-suspended in a 5ml RBC lysis buffer and incubated for 5 minutes at room temperature. Three millilitre was added after the incubation and then centrifuged for 5 minutes at 1200 rpm. The samples were then re-suspended in 1ml of medium and sieved through a 40µm sieve into a new 50ml tube, then centrifuged for 10 minutes at 1200 rpm. The cells were counted using 2% trypan blue using 1 in 10 dilution.

2.10. **Antibodies and Flow cytometry Analysis**

2.10.1. **Surface staining**

A total of 2 000 000 cells per 200µl of medium (IMDM supplemented with 10% iFBS and 0.5% Pen-strep) from each of the samples was added into a V bottom plate (Nalge Nunc International, USA) and centrifuged for 5 minutes at 1500 rpm. The staining antibody cocktail was prepared containing facs buffer (% BSA and 1X PBS buffer), 2% heat inactivated rat serum (iRS), 1% FcγRIII plus the following combination of surface antibody markers also shown in Appendix 1.

CD45 (PE), Siglec-F (APC), F4/80 (PE-Cy7), 7AAD (PerCp Cy5.5), CD4 (FITCS), CD11b (V450), CD11c (A700), Ly6G (APC-Cy7), CD8 (V500).
And
Lin (PE), ICOS (APC), 7AAD (PerCp Cy5.5), T1ST2 (FITCS), CD45 (Texas red)

After centrifugation, the supernatant was discarded from the plate gently and the staining cocktail was added into each of the samples. The plates were then

covered with a foil and incubated for 30 minutes in 4^0C fridge. Two hundred microliters of Facs buffer was added into the samples and centrifuged for 5 minutes at 1500 rpm. The supernatant was discarded and the samples were re-suspended in 100µl of Facs buffer, then transferred into facs tubes for analysis on LSR Fortessa (BD Immunocytometry system, USA). The samples were analysed using FlowJo software (Treestar, USA).

2.10.2. **Intra-cellular staining**

2.10.2.1. *Ex-vivo* re-stimulation

A mixture containing 500µl of medium (IMDM supplemented with 10% iFBS and 0.5% Pen-strep), 2.5µl of 50ng/ml Phorbol 12-myristate 13-acetate (PMA), 2.5µl of 250ng/ml Ionomycin, and 2µl of 200µM Monensin were prepared. Ten microliters of the mixture was added into the wells of a new sterile flat bottom plate (Nalge Nunc International, USA) and about 200µl of the cell suspension containing $2x10^6$ cells was also added to the mixture in the plate. The plate was then incubated for 8 hours in 37^0C incubator.

2.10.2.2. Staining

The re-stimulated cell suspension (≥200µl) was transferred from the flat bottom plate and into a new sterile V bottom plate and then centrifuged for 5 minutes at 1500rpm. The supernatant was gently discarded and added 50µl of the 1^{st} staining antibody cocktail containing facs buffer (% BSA and 1X PBS buffer), 2% heat inactivated rat serum (iRS), 1% FcγRIII plus the following combination of antibody markers also shown in Appendix 1. CD4 (FITCS), CD11b (V450), CD3 (A700), CD8 (V500). CD45 (Texas red).

The plates were covered with a foil and incubated for 30 minutes at 4^0C fridge. Two hundred microliters of Facs buffer was added into the samples and centrifuged for 5 minutes at 1500 rpm. The supernatant was discarded and the samples were re-suspended in 100µl ice-cold 1x PBS buffer. Then 100µl of 4% Paraformaldehyde (PFA) was added to the samples and incubated on ice in dark

for 60 minutes. After incubation, 200µl of ice-cold 1x PBS buffer was added. The samples were then centrifuged for 5 minutes at 1500 rpm and gently discarded the supernatant. The samples were re-suspended in 200µl of permeabilization buffer. Again the samples were incubated on ice in dark for 60 minutes and then centrifuged for 5 minutes at 1500 rpm. They were then re-suspended in 50µl of staining cytokine cocktail containing 1x 2% heat inactivated rat serum (iRBS), 1% FcγRIII plus the following combination of antibody markers also shown in Appendix 1.

IL-5 (PE) , IL-13 (PE-Cy7), IL-4 (PerCp Cy5.5), IL-17 (APC-Cy7),

The samples were incubated on ice in dark for 60 minutes and then added 200µl of permeabilization buffer. The samples were centrifuged for 5 minutes at 1500 rpm and then re-suspended in 100µl of facs buffer and transferred into facs tubes for analysis on LSR Fortessa.

2.11. *Ex-vivo* re-stimulation for cytokine analysis

All the reagents used in this experiment were sterile and the work was carried out in a sterile environment. One flat bottom plate (Nalge Nunc International, USA) was coated with 50µl of medium (IMDM supplemented with 10% iFBS and 0.5% Pen-strep) containing 20µg/ml anti-CD3 and incubated for 2 hours in a 37^0C incubator. After incubation, the supernatant was gently removed and 100µl of cell suspension containing 10^6 cells was added. In another flat bottom plate, 100µl of 20µg/ml *S. mansoni* soluble egg antigen (SEA) dissolved in medium (IMDM supplemented with 10% iFBS and 0.5% Pen-strep) was added together with 100µl of cell suspension containing 10^6 cells. In a 3rd plate, 100µl of medium (IMDM supplemented with 10% iFBS and 0.5% Pen-strep) was added together with 100µl of cell suspension containing 10^6 cells. The three plates were incubated in 37^0C incubator for 72 hours and then stored in -80^0C freezer.

2.12. **Preparation of Tissue homogenates**

2.12.1. **Liver and gut**

The samples were thawed on ice and 500µl of extraction buffer (1X PBS buffer with 1:100 dilution of protease inhibitor, and 0.1% Tween) was added to each of the samples. The samples were then homogenized using 5mm stainless steel bead for 5 minutes with break intervals after each 1 minute (5x 1 minute) allowing the samples to be completely homogenized. Another 500µl of the extraction buffer was added and the samples were centrifuged for 5 minutes at 4800 rpm in a 4^0C. The supernatant was then transferred into new labelled 2ml Eppendorf tubes and the protein content of each sample was measure using BCA assay (Thermo Scientific, USA) then stored in -80^0C until they were needed for further analysis. BCA assay was carried out according to manufacturer's instructions to determine protein content (Thermo Scientific, USA. Catalog number 23225).

2.13. **Serum collection from whole blood**

The blood samples collected in blood collection tubes (Microtainer, BD, USA) were centrifuged for 15 minutes at 8000 revolutions per minute (rpm) to separate out the serum from whole blood and stored in -80^0C freezer until needed.

2.14. **Enzyme-Linked Immunosorbent Assay (ELISA) Analysis**

2.14.1. **Cytokine analysis**

Cytokine responses were measured in serum, MLN stimulated either with 20µg/ml of SEA or 20µg/ml of anti CD3, liver & gut homogenates from non-infected and infected mice. Ninety six well plates (Nalge Nunc International, USA) were coated with primary capture antibodies specific for each cytokine of

interest. The capture antibodies diluted in 1X PBS buffer were used - Refer to Appendix 2.

The plates were incubated overnight in 4^0C fridge, and then washed with wash buffer (20g KCl, 20g $KH_2HPO_4.2H_2O$, 800g NaCl, 50ml Tween-20, dissolved in 5 litre, then diluted 1:20 in ddH_2O) 3 times. The plates were blocked with 200µl of 2% milk powder then incubated for 2 hours in 37^0C. The plates were washed again with wash buffer 5 times and then added 50µl of samples together with recombinant standards for each cytokine tested. In the case of TGF-β, 48µl of samples plus 2µl of 1M HCl pH 3 and left to incubate for 1 hour in 4^0C. The reaction was stopped by adding 2µl of 1M of NaOH. All the plates were then incubated overnight in 4^0C. The recombinant proteins were used as standards - Refer to Appendix 2.

After overnight incubation, the plates were washed again in wash buffer 5 times. Secondary biotinylated antibodies were then added to the appropriate plates for each of the test cytokines and incubated the plates for 2 hours in 37^0C. The plates were then washed 5 times using wash buffer and then added strep-avidin substrate conjugated with either alkaline phosphatase (AP) in 1/1000 dilution. The plates were incubated for 1 hour in 37^0C and then washed the plates again 5 times using wash buffer. The plates were then developed by adding 1mg/ml of 4 Nitrophenyl phosphate disodium salt hexahydrate (PNP) (Merck, Germany) diluted in AP substrate buffer into each well of the plates. The plates were again incubated for 10 minutes in 37^0C to allow for colour development in positive samples, and the optical density (OD) was measured on a VERSAmax microplate reader (Molecular devices, USA).

2.14.2. **Antibody analysis**

Antibody response was measured in blood serum samples collected from non-infected and infected mice. The 96 well plates (Nalge Nunc International, USA) were coated with 10µg/ml of SEA overnight at 4^0C. The plates were then washed

3 times using wash buffer and then blocked with 2% milk powder for 2 hours in 37^0C. The plates were washed 5 times and serum samples were then added in a 10-fold dilution series. In the case of IgE, the samples were not diluted and the standard for the antibody was also included. The plates were then incubated overnight in 4^0C then washed 5 times using wash buffer. The plates were incubated for 2 hours in 37^0C with phosphatase-conjugated secondary detection antibodies for IgE. The plates were then developed using 1mg/ml of 4 Nitrophenylphosphate (PNP) (Sigma-Aldrich, Germany) diluted in AP substrate buffer and incubated for 10 minutes in 37^0C. The OD was measured on a VERSAmax microplate reader (Molecular devices, USA).

2.15. **Quantification of liver enzymes in the serum ALT and AST analysis**

Serum samples were diluted by 1:20 in sterile 0.9% Saline solution and then submitted to the National health Laboratory Services for further analysis.

2.16. **Hydroxyproline Assay**

The hydroxylproline content was measured in liver and gut tissues collected from non-infected and infected mice. The tissue were first weighed and then transferred into clean glass screw cap tubes containing 5ml of 6M HCl and incubated overnight at 110^0C incubator. The samples were topped up to 10ml by adding 5ml of double distilled water (dH_2O) and then mixed by vortex. Two millilitre of each sample was filtered through Whitman No.1 filter paper (Sigma-Aldrich, Germany) into new labelled 15ml falcon tubes. One drop of 1% phenolphthalein in ethanol was added into each of the tubes containing 2ml filtrate. A few drops of 10M NaOH were added into each filtrate sample until a colour change from light brown to pink was observed. A few more drops of 3M HCl were added to titrate the samples back to light brown and then topped up to 4ml using dH_2O. From each of the samples, 200µl was transferred into new 15ml falcon tubes and the OH-proline standards were prepared in a 2-fold dilution starting from 200µg/ml into each of the samples and standards, 400µl of

isopropanol was added and were mixed using vortex. Two hundred microliters of solution A was added into each tube and mixed, then incubated at room temperature for 10 minutes. Two and a half millilitres of solution B was added into the samples and mixed by vortex then incubated for 25 minutes in 60^0C water bath. The samples were immediately cooled in ice cold water then transferred 200µl of each of the samples into 96 well plates (Nalge Nunc International, USA). The samples' OD was read using VERSAmax microplate reader (Molecular devices, USA) at wavelengths 558 nm (excitation) and 570 nm (emission).

2.17. **Histology**

Tissue samples (Liver and Gut) were fixed in neutral buffered formalin and processed, and about 5µm sections were stained with hematoxylin and eosin (H&E) or Chromotrope aniline blue (CAB). The diameters of each granuloma containing a single egg were measured using a computerized morphometry analysis program. The egg diameter were then subtracted from the diameter of the whole granuloma. A total of 100 granulomas per group of mice were measured for analysis. Tissue samples (Liver and Gut) fixed in neutral buffered formalin and processed were also stained with Chromotrope aniline blue (CAB) in order to measure fibrosis.

2.18. **Parasitaemia/egg burden determination.**

Tissue samples (Liver, Lung, and Gut) collected were processed for egg burden analysis. Briefly, the samples were incubated in 15ml tubes containing 5ml of 5% potassium hydroxide (KOH) overnight in a 37^0C incubator. The samples were then centrifuged for 10 minutes at 2000 revolutions per minute (rpm) and 3 ml of supernatant were discarded. The remaining supernatant was re-suspended using a vortex for 15 seconds and the 50µl of the sample was viewed under a dissecting microscope to count the number of eggs lodging the tissues.

2.19. **Statistical analysis**

The values presented in this work are shown as mean ± SEM and significant differences were determined using the unpaired one or two---tailed Student's t---test. *, ** and *** indicate $p<0.05$, $p<0.01$ and $p<0.001$ respectively (GraphpadPrism™).

3. Results:

3.1. BATF2 sustained/ increased expression in egg-harbouring tissues during experimental schistosomiasis.

The study initially assessed the expression of BATF2 at homeostasis in liver and intestinal tissues, and also assessed how Schistosomiasis infection alters the expression of this transcription factor in these organs given the preferential, if not exclusive retention of *S. mansoni* eggs in these tissues. In order to asses this, RNA was isolated from livers and guts of naïve and *S. mansoni* infected wild type (129SvEv) mice and reversed transcribed into cDNA. The BATF2 expression was then quantified by qPCR with HPRT primers as housekeeping gene. The expression of BATF2 was considerably higher in the liver when compared to the intestine (Figure 5, filled circles). Interestingly, 7 weeks post infection with *S. mansoni*, the expression of BATF2 significantly increased in the liver of infected animals, while the expression remained unchanged in the gut of the infected (Figure 5, open circles). We therefore concluded that BATF2 expression is sustained, thus possibly required in the liver and gut of mice during experimental schistosomiasis.

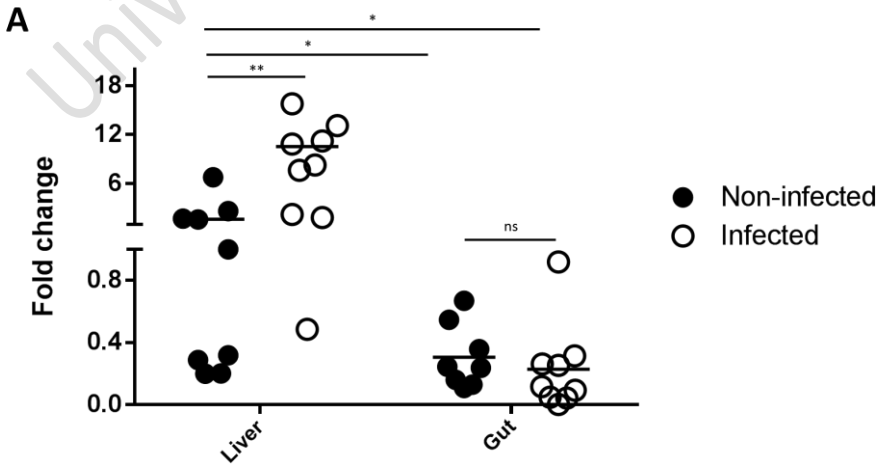

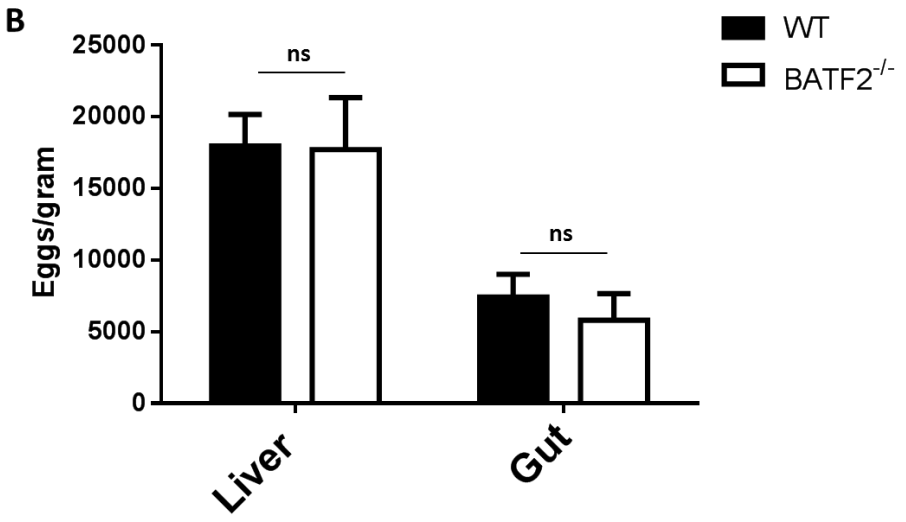

Figure 5: **BATF2 expression in egg-infested tissues during experimental schistosomiasis**. (A) BATF2 mRNA expression levels in liver and gut tissues from naïve (closed circles) and *S. mansoni* infected (open circles) mice measured using qPCR normalised to HPRT mRNA control. (B) Quantification of egg burden the liver and gut of WT (black bar) and BATF2 deficient (white bar) mice. The data presented included a sample size of n= 8 - 10 mice per group. *p< 0.05, **p< 0.01, and ***p<0.001 vs non-infected using one tailed student's t-test.

3.2. No major physiological impairment in BATF2 deficient mice at homeostasis, despite a minimal disturbance of immune cell distributions.

To interrogate the need for BATF2 expression in the liver and gut during experimental schistosomiasis, we made use of a murine BATF2 deficient 129SvEv mouse model. The removal of BATF2 expression in these mice was confirmed through PCR using the following primers: BATF2 P1 (5'-ACC CTC CAC CAT CCT TCT TC), BATF2 P2 (5'- GAC TGG TCT GCA GTG TGA GC), BATF2 P3 (5'- CCA GCT CAT TCC TCC CAC T). The BATF2 P1 and P3 primers were used to identify the presence of an intact functional BATF2 gene while BATF2 P1 and P3 were used to identify the truncated non-functional BATF2 gene. As shown in figure 6 BATF2 deficient mice had a non-functional truncated BATF2 gene unlike the wild type mice.

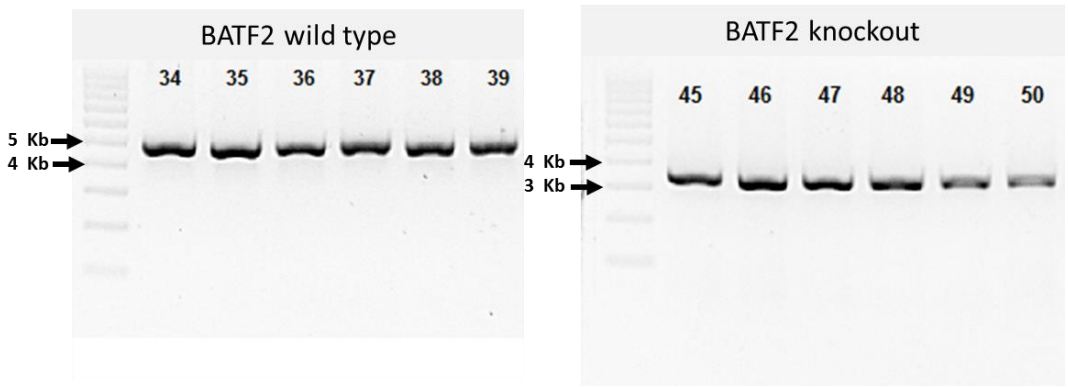

Figure 6: Genotyping of BATF2 mice to confirm the removal of BATF2 expression in 129SvEv mice.

The body (Figure 7A) and organ weights (Figure 7B) which included liver, spleen and heart of the 129SvEv WT and BATF2 deficient (BATF2$^{-/-}$) mice were compared to identify any physiological impairment of the mice in the absence of BATF2 expression. The intestinal length was also measured from the stomach to the caecum (Figure 7C). Although most of the organs were not affected, the intestinal length (from stomach to caecum) was reduced indicating a possible role of BATF2 in maintaining the integrity of this tissue.

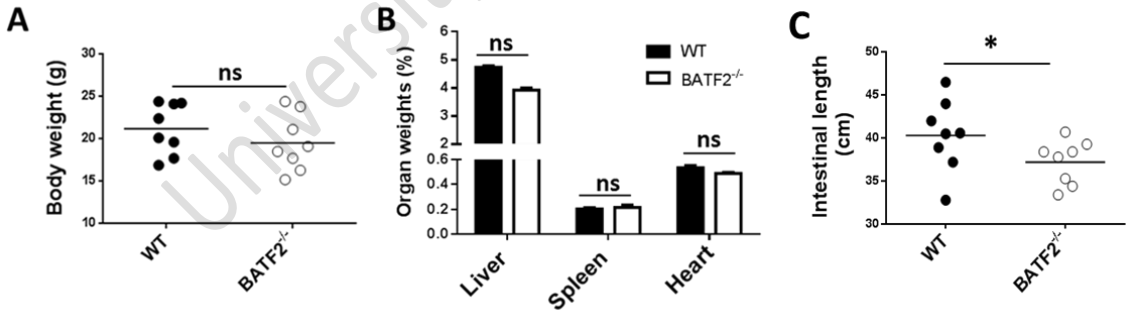

Figure 7. The absence of BATF2 results in reduced intestinal length with no effect on body and organ weights at homeostasis. (A) Summary of body and (B) organ weights in relation to body weight. (C) Quantification of intestinal length (from base of stomach to caecum). The data presented included a sample size of n= 8 - 10 mice per group. *p< 0.05, **p< 0.01, and ***p<0.001 vs WT using one tailed student's t-test.

The organs from the BATF2 deficient mice were further analysed for any signs of hepatoxicity by measuring serum levels of alanine transaminase (ALT) and aspartate transaminase (AST) (Figure 8). We noted no elevation of liver enzyme levels in the sera of BATF2 deficient mice when compared to the littermate control mice (Figure 8).

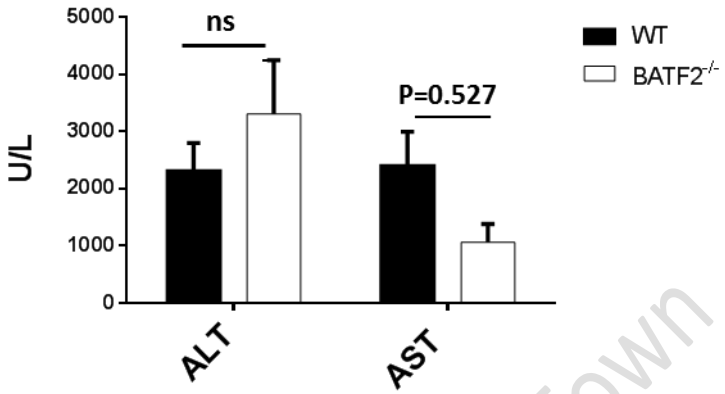

Figure 8. The absence of BATF2 does not majorly affect tissue damage at homeostasis. Quantification of serum levels of alanine transaminase (ALT) and aspartate transaminase (AST) in WT (black bars) and BATF2 deficient (white bars) mice. The data presented is from two independent experiments which included a sample size of n= 8 - 10 mice per group. *p< 0.05, **p< 0.01, and ***p<0.001 vs WT using one tailed student's t-test.

Furthermore, BATF2-deficient mice were analysed for any cellular impairment at homeostasis. The cellularities of thymus, spleen, mesenteric lymph nodes and guts were defined (Figure 9). In as much as we noted a minimal reduction in total mesenteric lymph node cell numbers in BATF2-deficient mice (Figure 9), no major alteration of the total cell numbers was observed overall in other analysed tissues (spleen, thymus and gut) when compared to littermate control mice.

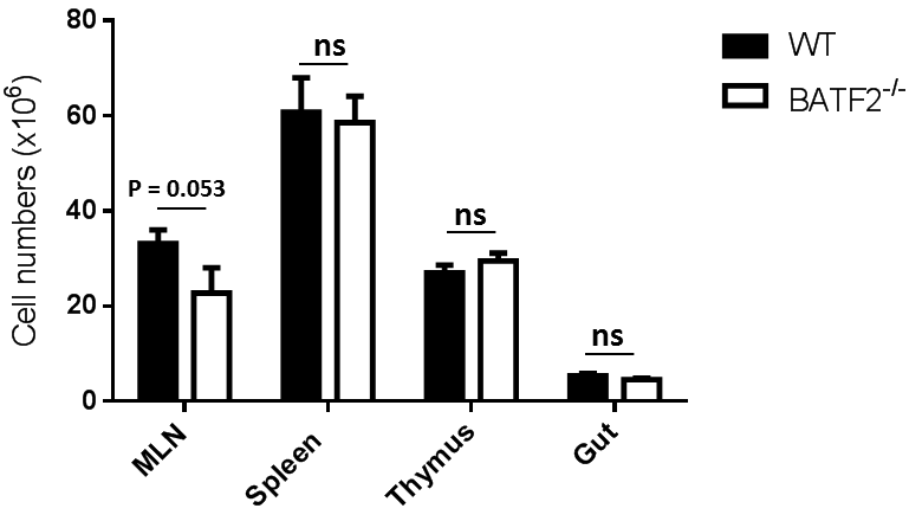

Figure 9. The absence of BATF2 had no major influence on the organ cellularity in 129SvEv mice at homeostasis. Organ cellularities between WT and BATF2 deficient mice. The data presented included a sample size of n= 8 - 10 mice per group. *p< 0.05, **p< 0.01, and ***p<0.001 vs WT using one tailed student's t-test.

An in-depth analysis of the cell type distribution in the thymus, spleens, MLNs and guts of BATF2 deficient mice was then conducted to further assess the effect of BATF2 deficiency on immune cell distribution at homeostasis. Single cell suspensions were obtained from each of the organs and were analysed by Flow cytometry to identify immune cell populations. Figure 10 shows the gating strategy used to identify the various lymphoid and myeloid cell types analysed.

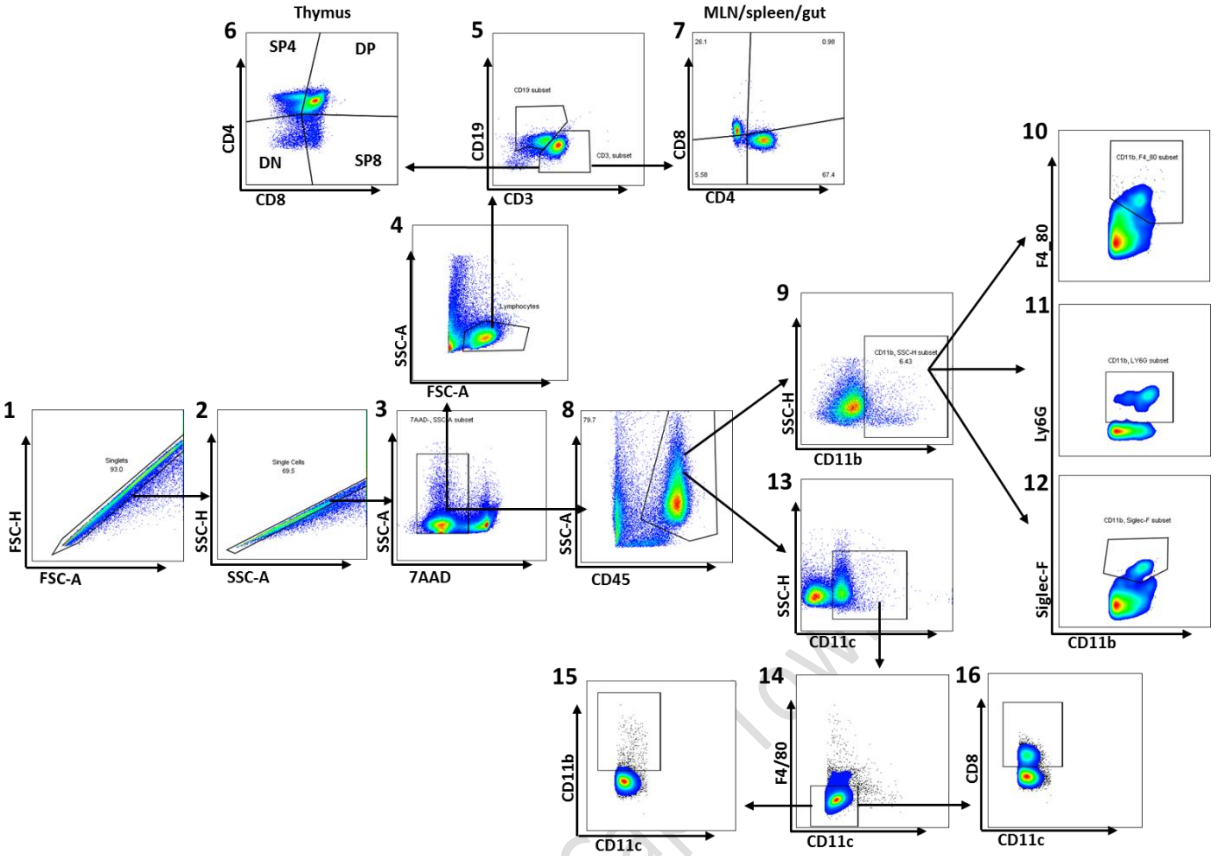

Figure 10. Gating strategy used from flow cytometry to identify and quantify lymphocytes and myeloid cells. (1) The cells are first gated out from the singlets and (2) single cells to rule out doublet cell populations and those with disproportional sizes. (3) Live cells were then gated on 7AAD negative population with (4) lymphocytes being identified from FSC-A high and SSC-A low. From the lymphocytes, (5) T cell (CD3+ CD19-) and B cell (CD19+ CD3-) lymphocytes were gated out and further characterised into (6) DN (CD4- CD8-), SP4 (CD4+ CD8-), DP (CD4+ CD8+), and SP8 (CD4- CD8+) in the case of thymus. (7) In MLN, spleen, and gut the T cells were further characterised into CD4+ and CD8+ T cells. (8) Myeloid cells were identified as SSC-A high and CD45+ gated from the 7AAD- population. From the myeloid population, (9) CD11b+ population was gated on in order to identify (10) macrophages (CD11b+ F4/80+), (11) neutrophils (CD11b+ Ly6G+), and (12) eosinophils (CD11b+ Siglec-F+). Another population that was gated from the myeloid population was the (13) CD11c+ population which represents the majority of dendritic cells. From this CD11c+ population the (14) dendritic cells (CD11c+ F4/80-) were gated. Two subtype populations of the dendritic cells were further identified within the DC population, namely (15) CD11b+ CD11c+ DCs and (16) CD8+ CD11c+ DCs.

As depicted in Figure 11 below, the frequencies of lymphocyte and myeloid cell populations in thymus MLN, spleen, and the intestinal tissue in wild type and BATF2 deficient mice were determined. In the thymus (Figure 11A), absence of

BATF2 resulted in a reduced frequency of double negative (CD4- CD8-) immature thymocytes which, counterintuitively, did not affect the frequencies of DP and SP thymocytes (Figure 11A), or the overall number of thymocytes (Figure 11A). In the case of the mesenteric lymph nodes (Figure 11B), we noted no alteration of the frequencies of the analysed T cell, macrophages or neutrophils in BATF2 deficient mice at homeostasis (Figure 11B). However, a reduction of CD8+ and CD11b+ dendritic cells was apparent in BATF2 deficient mice (Figure 11B). Conversely, T cells were less represented in the spleens and guts of BATF2 deficient mice (Figure 11C and Figure 11D). We also noted that the frequencies of splenic and intestinal neutrophils and intestinal macrophages were altered in BATF2 deficient mice (Figure 11C and Figure 11D). Together, our data argue for a possible regulatory role of BATF2 in regulating major immune cell frequencies

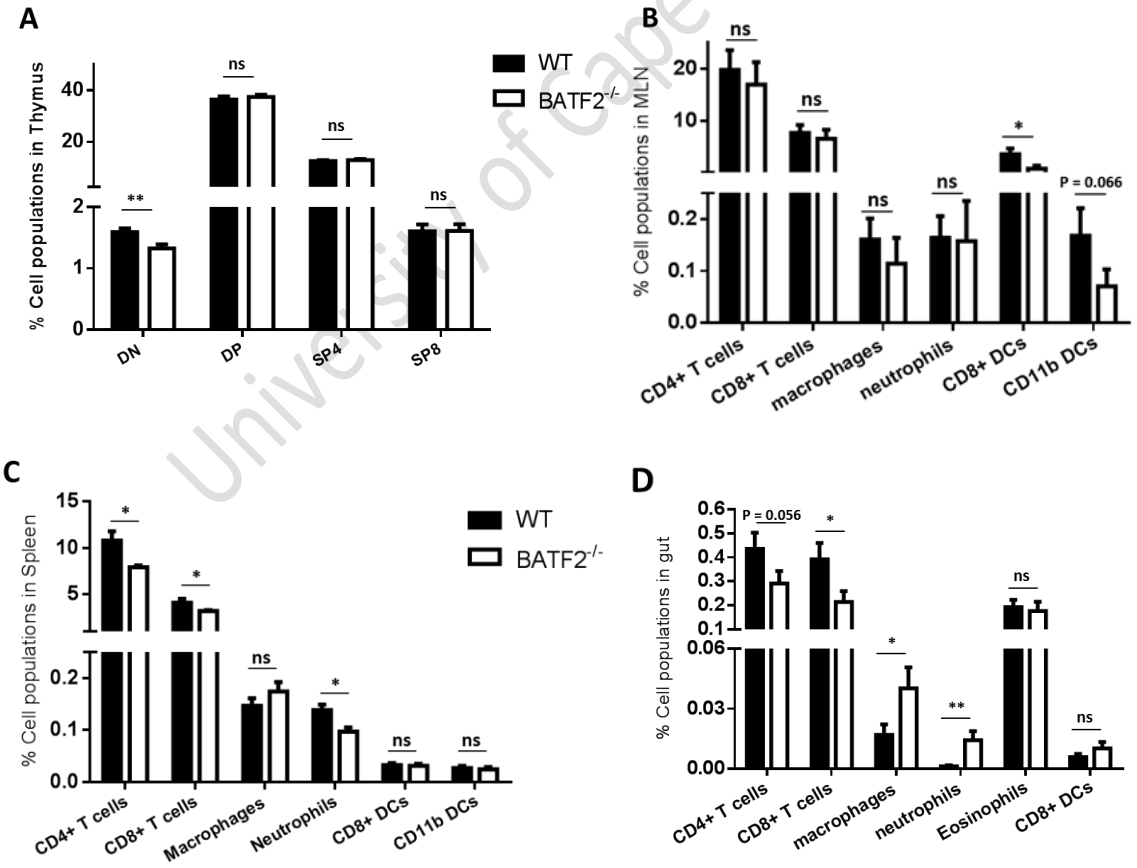

Figure 11. BATF2 deficiency on cell distribution at homeostasis. Frequencies of lymphocyte (CD3+ CD4+ T cells, CD3+ CD8+ T cells) and myeloid (CD11c+ F4/80- CD8+ DCs, CD11c+ F4/80- CD11b+ DCs, CD11b+ F4/80+ macrophages, Ly6G+ neutrophils, Siglec-F+ eosinophils)

populations in (A) thymus, (B) MLN, (C) spleen, and (D) intestinal tissue per group using Flow cytometry. The data presented is from two independent experiments which included a sample size of n= 8 - 10 mice per group. *p< 0.05, **p< 0.01, and ***p<0.001 versus WT using one tailed student's t-test.

We then questioned whether such altered immune cell distribution – mostly apparent in the gut tissue - might translate into an altered tissue immune response at homeostasis in the absence of BATF2. To address this, gut tissue specific cytokine concentrations were measured. . As shown in figure 12, the absence of BATF2 resulted in an elevated production of various cytokines (IL-1, IL-4, IL-5, IL-17, TNF-alpha, and TGF-beta) in the gut tissue (Figures 12). This indicated, unprecedentedly, that BATF2 Does play a negative regulatory role on cytokine release at homeostasis, particularly in the gut tissue.

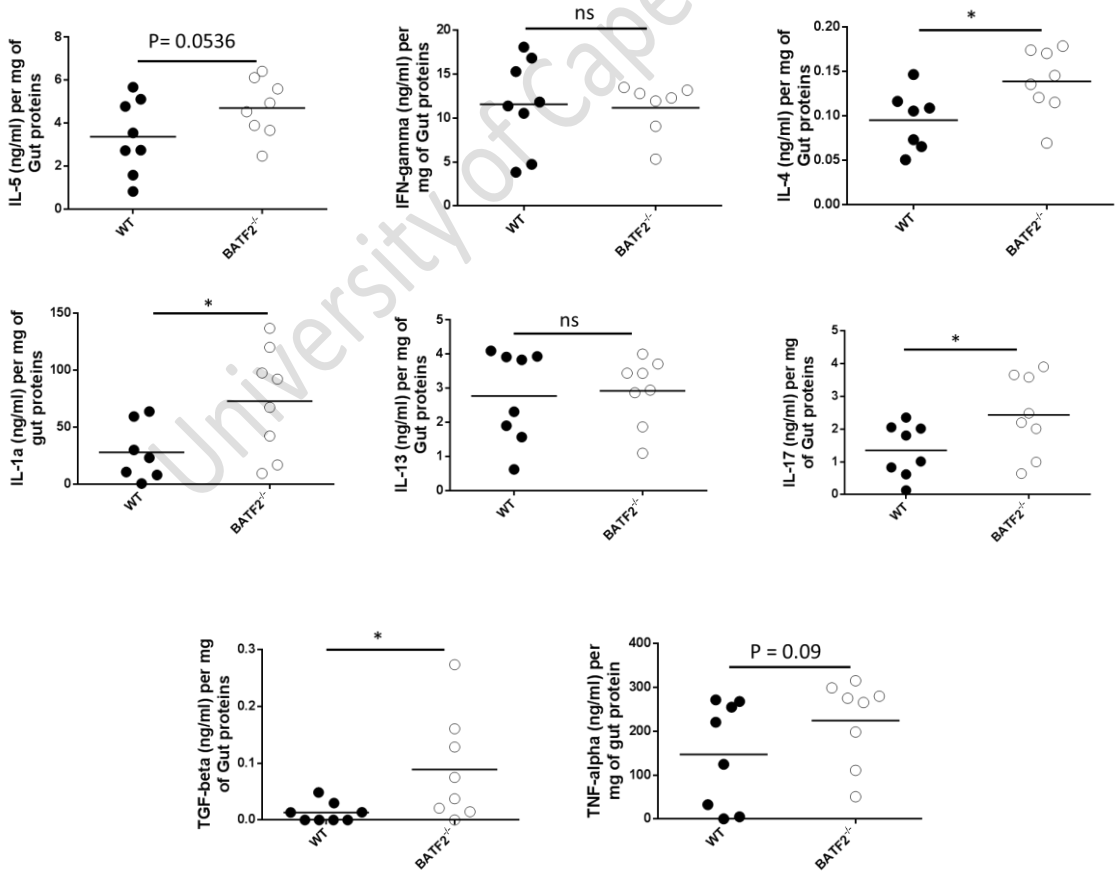

Figure 12. Increased cytokine production in the absence of BATF2 at homeostasis in the intestinal tissue. Quantification of intestinal tissue cytokine concentrations at homeostasis using

ELISA. The data presented included a sample size of n= 8 mice per group. *p< 0.05, **p< 0.01, and ***p<0.001 vs WT using one tailed student's t-test.).

We then addressed whether such elevated tissue cytokines would result in increased pathology. For this, we measured the hydroxyproline levels in the liver and intestinal tissue to indirectly assess the collagen content and fibrosis in the tissues (Figure 13). We noted no change at baseline of the levels of fibrosis in the liver and gut of naïve BATF2-deficient mice and littermate control. This indicated that BATF2 deficiency, does not aggravate gut fibrosis at homeostasis.

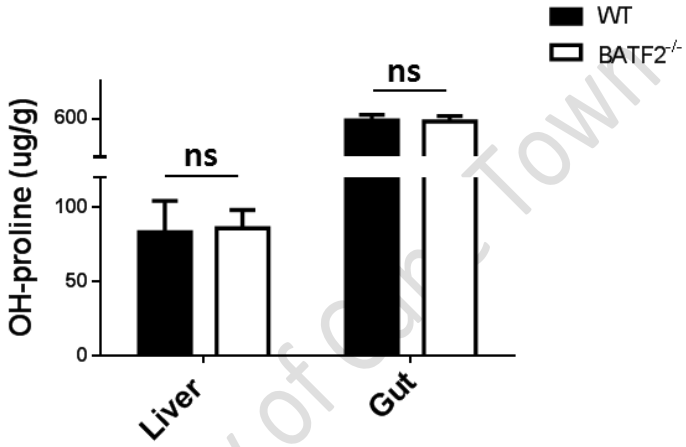

Figure 13. The absence of BATF2 had no significant influence on collagen content and thus tissue fibrosis at homeostasis. Quantification of hydroxyproline levels, as measures of collagen content and fibrosis in liver and intestinal tissues of WT (black bar) and BATF2 deficient mice (white bar). The data presented is from two independent experiments which included a sample size of n= 8 - 10 mice per group. *p< 0.05, **p< 0.01, and ***p<0.001 vs WT using one tailed student's t-test.

Finally, given such changes in the cellular distribution within organs of BATF2 deficient mice, which failed nonetheless to translate into heightened gut fibrosis when compared to littermate controls led us to question whether BATF2 deficiency might translate into an overall altered immune activation status in these mice. To address this, we measured total serum cytokine (Figure 14A, C, and D) and IgE levels (Figure 14B) and noted no difference between BATF2-deficient mice and littermate control serum cytokine levels (Figure 14A, C, and D). This indicated that despite the noted alteration of the quality of cellularity in

the thymus, spleens, MLNs and guts of BATF2-deficient mice, no systemic immune activation transpires as a result of BATF2 deficiency.

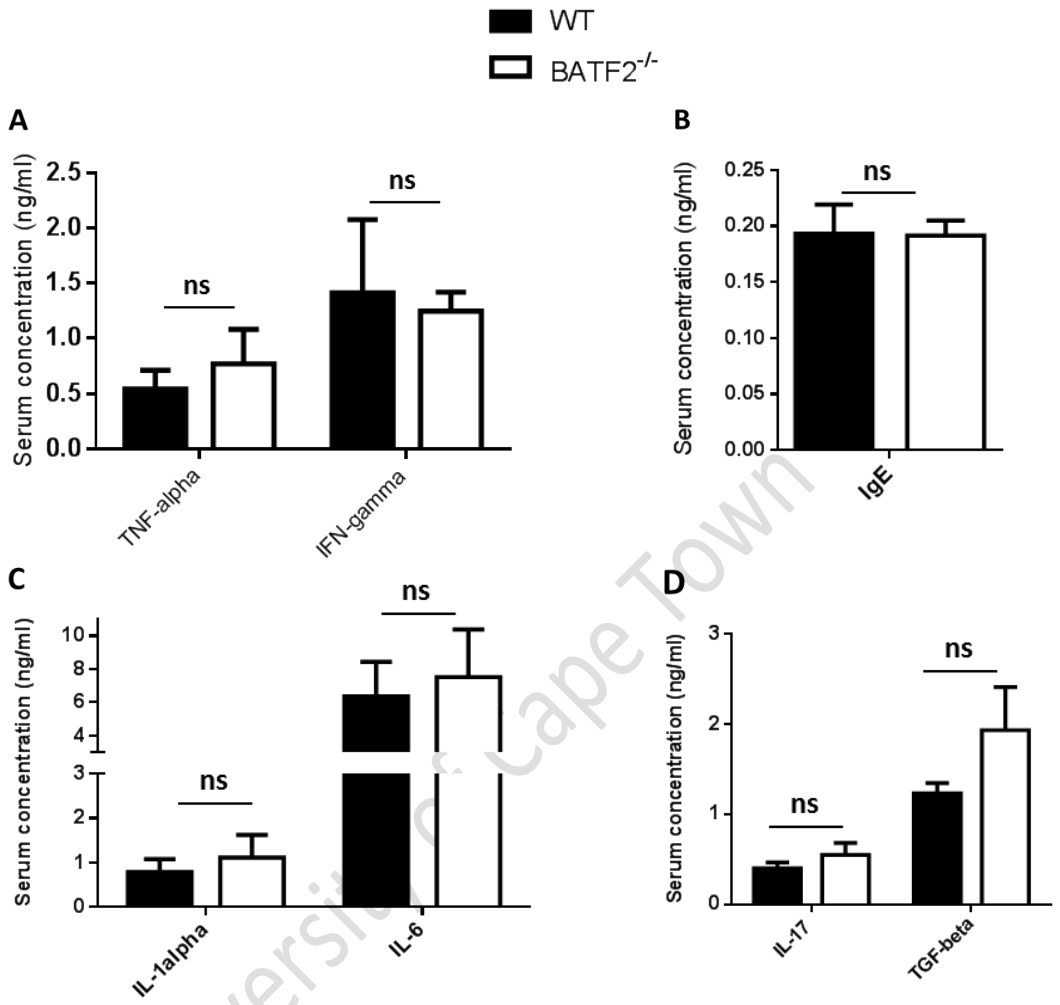

Figure 14. The absence of BATF2 does not affect serum cytokines and IgE levels at homeostasis. Quantification of serum cytokine and antibody concentrations at homeostasis using ELISA. The data presented included a sample size of n= 6 - 10 mice per group. *p< 0.05, **p< 0.01, and ***p<0.001 vs WT using one tailed student's t-test.

Overall, our data indicate that BATF2 deficiency at homeostasis does neither alter the animals' body weight nor the integrity of the liver, spleen, heart and gut (fibrosis) in a manner that has apparent clinical consequence in the BATF2-deficient mice.

3.3. **Increased pro-fibrotic immune response in the gut of *S. mansoni*-infected BATF2 deficient mice.**

Given that the BATF2 expression was confirmed in both the liver and the intestine during acute schistosomiasis. We then sort to understand what role the BATF2 could be playing in these tissues during acute schistosomiasis. BATF2 deficient mice and littermate controls were percutaneously infected with a dose of 80 live *S. mansoni* cercariae and culled for analysis 7 weeks post infection. Liver and gut tissues were the focus of our analysis as *S. mansoni* eggs reside in these tissues.

We first analysed immune cell dynamics as a result of *S. mansoni* infection in BATF2 deficient mice (Figure 15). We noted that *S. mansoni* infection led to a significant reduction of T cells in the liver of BATF2 deficient mice when compared to *S. mansoni* infected littermate controls. Of note, however, a reduction of macrophages and eosinophils paralleled by a considerable expansion of CD8+ DCs and T cells (both CD4+ and CD8+) was observed in the gut of *S. mansoni*-infected BATF2 deficient mice (Figure 15B).

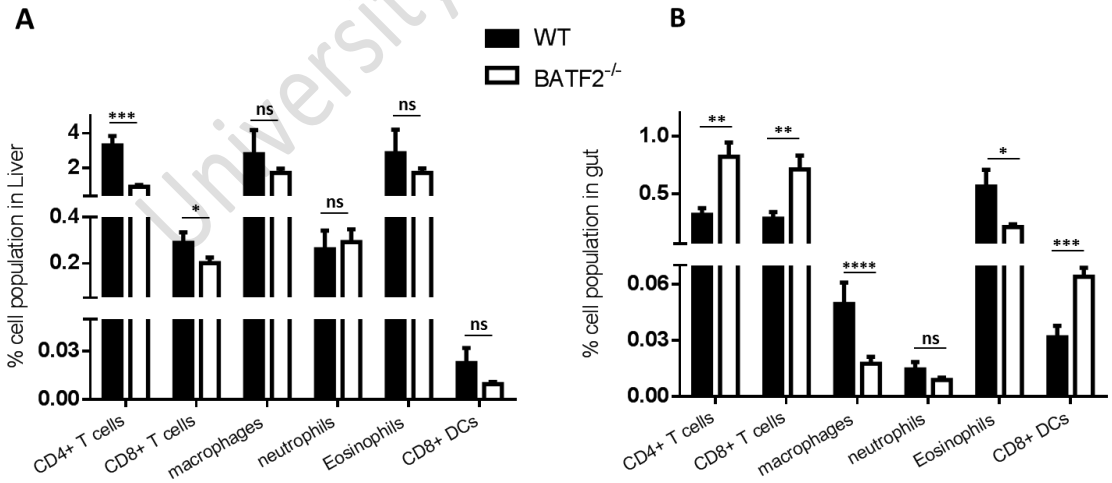

Figure 15. Immune cells distribution in the liver and the intestinal tissue of BATF2 deficient mice during schistosomiasis. Frequencies of lymphocyte (CD3+ CD4+ T cells, CD3+ CD8+ T cells) and myeloid (CD11c+ CD8+ DCs, CD11c+ CD11b+ DCs, CD11b+ F4/80+ macrophages, Ly6G+ neutrophils, Siglec-F+ eosinophils) populations in liver (A) and intestinal tissue (B) using Flow cytometry. The data presented included a sample size of n= 8 mice per group. *p< 0.05, **p< 0.01, and ***p<0.001 vs WT using one tailed student's t-test.

T-cells are instrumental in defining the immune properties thus pathological course of schistosomiasis. To address the functional nature of the expanded T cells in the parasitized tissues of *S. mansoni*-infected BATF2 deficient mice, we further performed intracellular cytokine detection (Figure 16). Whereas a drastic reduction of cytokine production was noted in liver CD4+ T cells from *S. mansoni*-infected BATF2 deficient mice when compared to infected littermate control liver CD4+ T cells (Figure 16A), gut CD4+ T-cells from *S. mansoni*-infected BATF2 deficient mice display a robustly elevated production of pro-fibrotic cytokines i.e. IL-5, IL-13 and IL-17 but not IL-4 when compared to gut CD4+ T cells from littermate controls (Figure 16B).

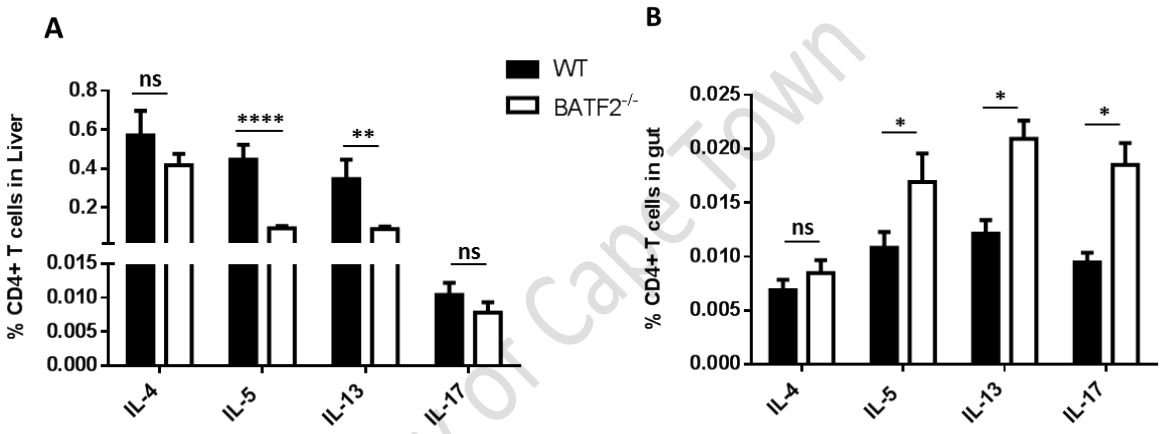

Figure 16. Increased pro-fibrotic CD4+ T cells in the gut while reduced in the liver. Frequency of cytokine producing CD4+ T cells from single cell suspension if liver (A) and intestine (B). The data presented included a sample size of n= 8 mice per group. *p< 0.05, **p< 0.01, and ***p<0.001 vs WT using one tailed student's t-test

Interestingly the profile was similar for CD8+ T cells where an increased production of pro-fibrotic cytokines (IL-5, IL-13, IL-17) was apparent in the gut of *S. mansoni*-infected BATF2 deficient mice when compared to Gut CD8+ T cells from littermate controls (Figure 17B).

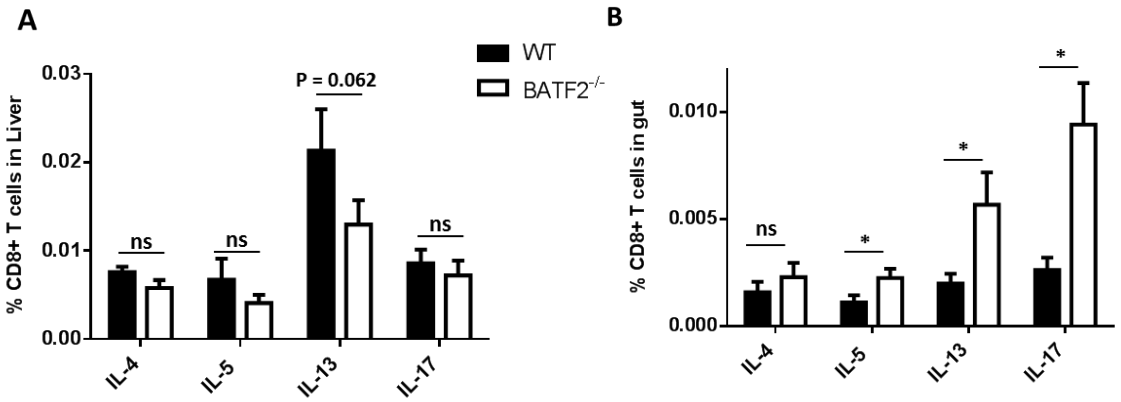

Figure 17. Increased pro-fibrotic CD8+ T cells in the gut. Frequency of cytokine producing CD8+ T cells from single cell suspension if liver (A) and intestine (B). The data presented included a sample size of n= 8 mice per group. *p< 0.05, **p< 0.01, and ***p<0.001 vs WT using one tailed student's t-test.

Altogether our findings demonstrate that BATF2 deficiency during schistosomiasis leads to an expansion of pro-fibrotic cytokine-producing T cells in the gut but not the liver in *S. mansoni*-infected BATF2 deficient mice.

We looked deeper on our observations and assessed the levels of liver and gut tissue cytokines. Besides, IL-5 which was increased in the liver of *S. mansoni*-infected BATF2 deficient mice when compared to littermate controls (Figure 18A), gut tissues from *S. mansoni*-infected BATF2 deficient mice showed a massive elevation in the production of TNF-alpha, IL-5, IL-13, TGF-beta and IL-17 all pro-fibrotic cytokines and pro-inflammatory IFN-gamma (Figure 18B). This observation reconciles with our intracellular cytokine profile in the gut of *S. mansoni*-infected BATF2 deficient mice and further suggests the elicitation of a strongly pro-fibrotic response specifically in the gut, but not the liver, of *S. mansoni*-infected BATF2 deficient mice.

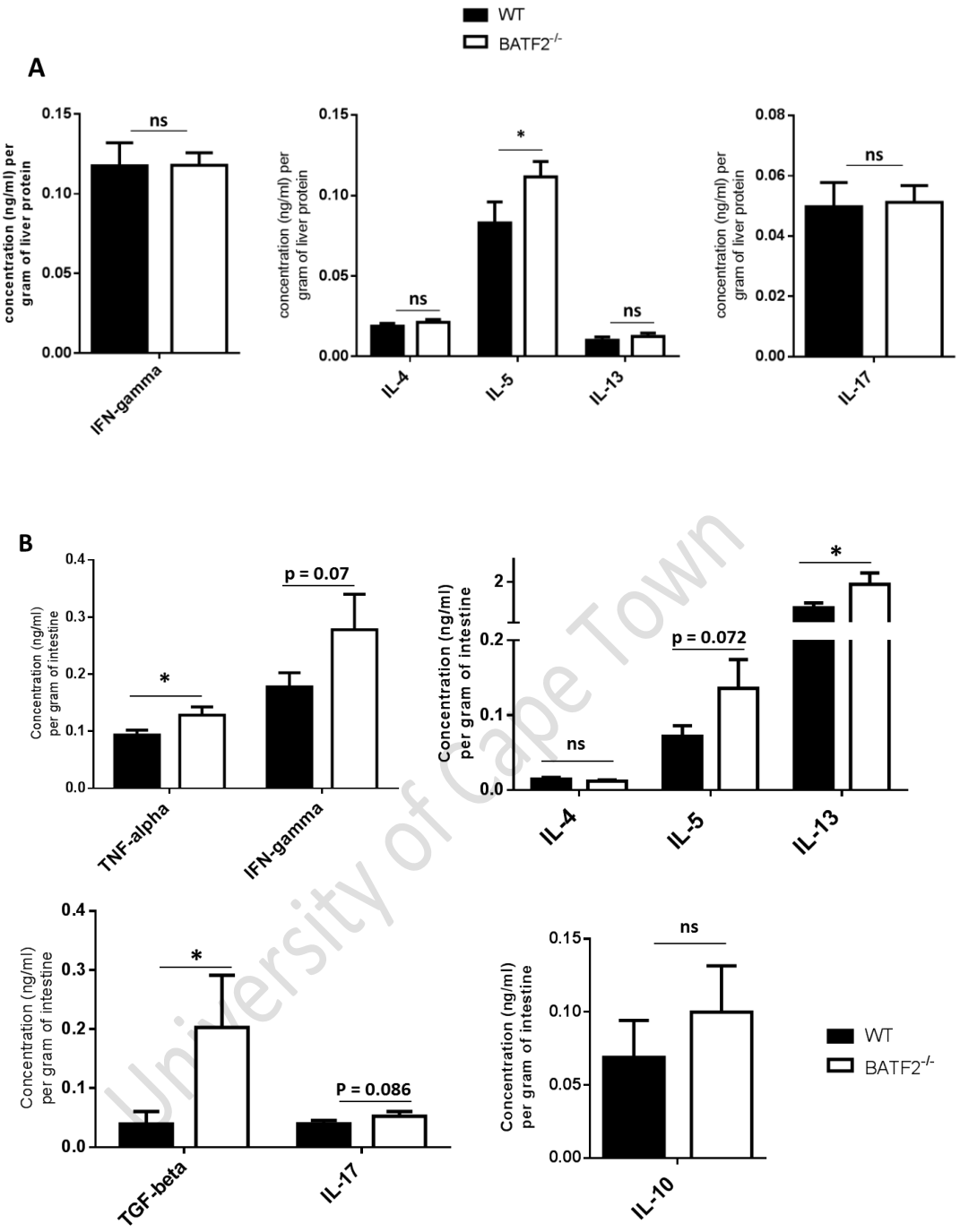

Figure 18. Increased pro-fibrotic and inflammatory cytokine profiles in the intestine in BATF2 deficient mice. Quantification of (A) liver and (B) intestinal cytokines using ELISA in WT (black bars) and BATF2 deficient mice (white bars). The data presented included a sample size of n= 8 mice per group. *p< 0.05, **p< 0.01, and ***p<0.001 vs WT using one tailed student's t-test.

3.4. Increased fibro-granulomatous inflammation in the gut of *S. mansoni*-infected BATF2 deficient mice.

Previous studies have shown that the development of extreme Th1, Th2, or Th17 cytokine producing phenotypes are highly detrimental during Schistosomiasis (Hoffman, 200; Rutitzky, 2007; Hammerich, 2010). The current study further aimed to understand how this observed increase in Th1, Th2, and Th17 responses continued to the gut would influence the egg-induced immunopathology in *S. mansoni*-infected BATF2 deficient mice.

First, the organ weights (spleen, heart and liver) of *S. mansoni*-infected BATF2-deficient mice were measured and compared to those of infected littermate controls (Figure 19). No significant differences in the organ weights were noted between *S. mansoni*-infected BATF2 deficient mice and those of the infected littermate controls (Figure 19).

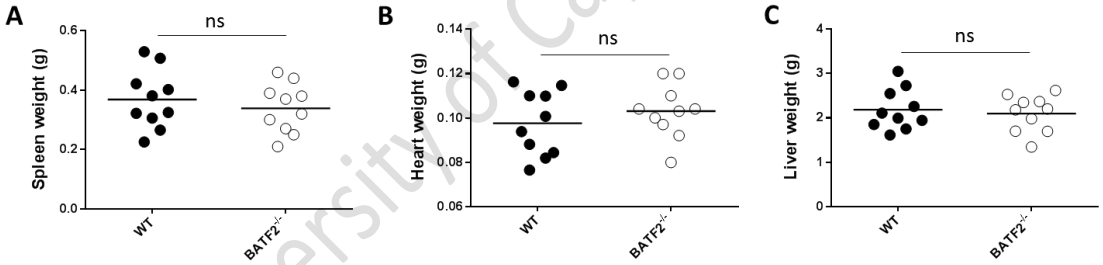

Figure 19. Organ weight in BATF2-deficient mice during schistosomiasis. Quantification of spleen (A), heart (A) and liver (D) weight. The data presented included a sample size of n = 10 mice per group. *p< 0.05, **p< 0.01, and ***p<0.001 vs WT using one tailed student's t-test.

To further appraise the pathology, Haematoxilin & Eosin staining of liver sections from *S. mansoni*-infected BATF2 deficient mice were analysed. We noted no noticeable significant alterations in the granuloma structure when compared with the wild type mice (Figure 20A). The area of the granuloma surrounding the *S. mansoni* egg, an indicator of the level of granulomatous inflammation was not affected in *S. mansoni*-infected BATF2 deficient mice when compared to infected littermate controls as determined by computational analysis on an automated microscope (Figure 20B).

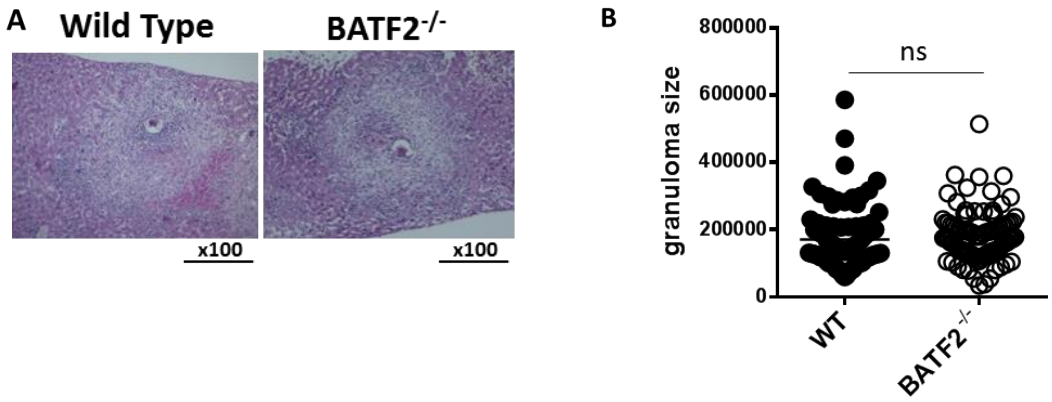

Figure 20. Absence of BATF2 does not affect the development of egg-surrounding granuloma in liver. Representative H&E staining of liver sections for morphological analysis of the tissue, and (F) quantification of granuloma area around each egg lodged in the tissue. 100 granulomas per group were included in the analysis. The data presented included a sample size of n = 8 - 10 mice per group. *p< 0.05, **p< 0.01, and ***p<0.001 vs WT using one tailed student's t-test.

We further stained liver sections with Chromotrope aniline blue (CAB) to assess the degree of fibrosis around the eggs logged in the liver tissue (Figure 21A). As shown in figure 21A, the blue staining intensity, representing collagen was reduced in liver sections of *S. mansoni*-infected BATF2 deficient mice when compared to liver sections from infected littermate controls. This was confirmed by measuring hydroxyproline levels in liver tissues (Figure 21B) showing reduced hydroxyproline levels in the liver tissue of *S. mansoni*-infected BATF2 deficient mice when compared to the levels reported from liver tissues from infected littermate controls (Figure 21B).

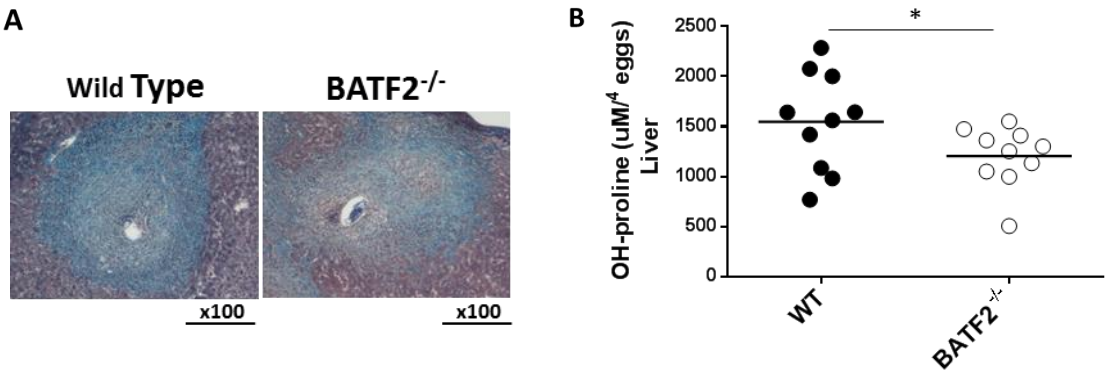

Figure 21. Liver fibrosis in BATF2-deficient mice during schistosomiasis. Representative CAB staining and (H) quantification of hydroxyproline levels normalised to egg numbers, as a measures of collagen content and fibrosis in liver. The data presented included a sample size of n = 8 - 10 mice per group. *p< 0.05, **p< 0.01, and ***p<0.001 vs WT using one tailed student's t-test.

Lastly, to assess hepatic pathology in our model, the hepatocellular damage was also measured by determining the serum levels of alanine transaminase (ALT) and aspartate transaminase (AST). Whereas the AST levels were not affected (Figure 22), the ALT levels were reduced strongly arguing against hepatotoxicity as a pathological feature ascribable to *S. mansoni*-infected BATF2 deficient mice when compared to infected littermate controls.

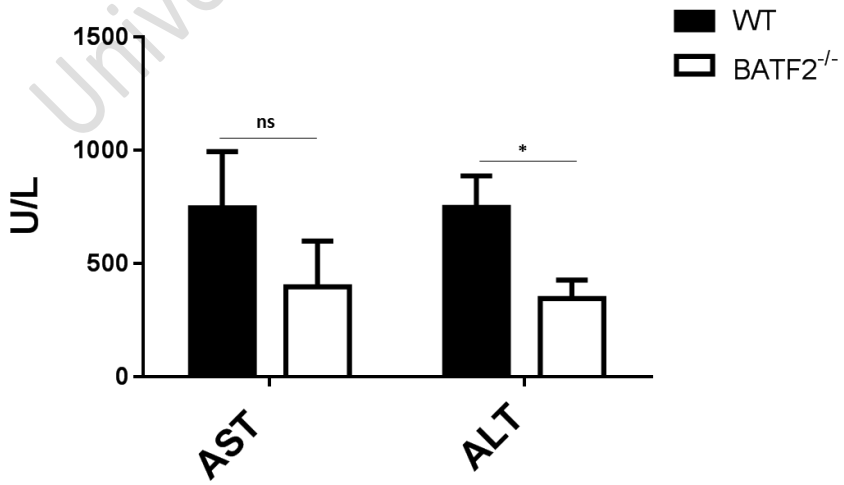

Figure 22. Reduced liver enzyme in BATF2 deficient mice during acute schistosomiasis. Analysis of hepatocellular damage measured by serum ratios of alanine transaminase (ALT) and aspartate transaminase (AST) The data presented included a sample size of n= 8 - 10 mice per group. *p< 0.05, **p< 0.01, and ***p<0.001 vs WT using one tailed student's t-test.

Next, the gut immunopathology was analysed. First the intestinal tissue length was measured as an indicator of the alteration of the gut function (Weaver, 1991). When comparing S*. mansoni*-infected BATF2 deficient mice to infected littermate controls, we noted an increased intestinal (Figure 23A) and colonic length (Figure 23C) in *S. mansoni*-infected BATF2 deficient mice.

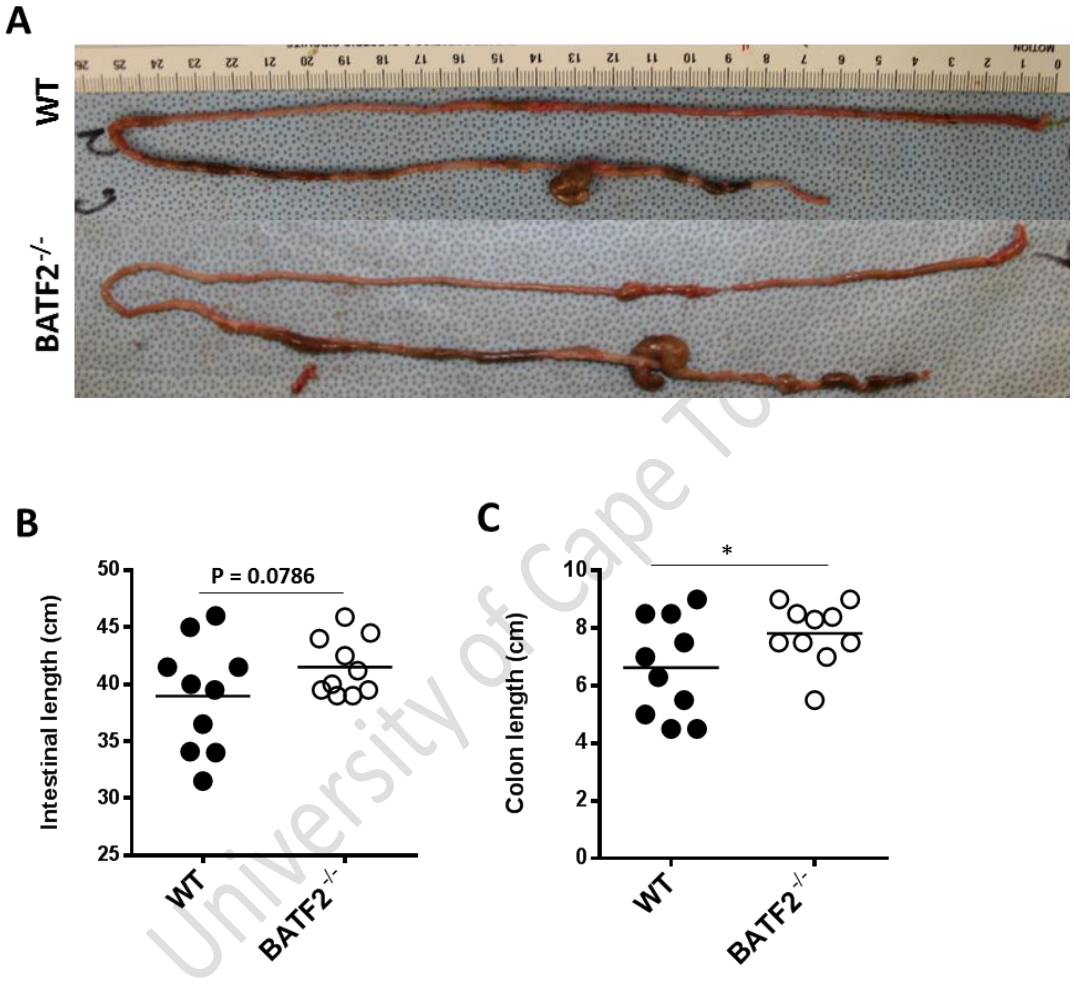

Figure 23. Increased intestinal and colon length in BATF2 deficient mice during acute schistosomiasis. Representative (A) and quantification of (B) intestinal length (from base of stomach to caecum) and (C) colon length. The data presented included a sample size of n= 10 mice per group. *p< 0.05, **p< 0.01, and ***p<0.001 vs WT using one tailed student's t-test.

To substantiate such an observation, the total gut cellularity was determined (Figure 24). We reported a strong trend of increased total gut cells in *S. mansoni*-infected BATF2 deficient mice further supporting the increased gut length reported in these mutant mice during schistosomiasis.

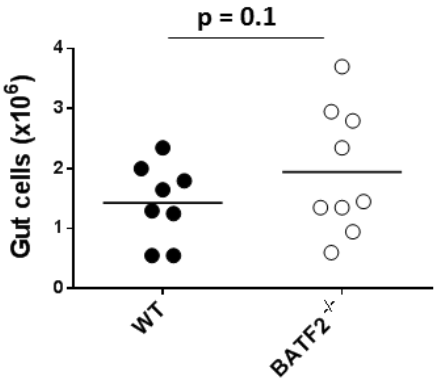

Figure 24. Intestinal cellularity in BATF2 deficient mice during schistosomiasis. Quantification of gut cellularity between wild type and BATF2 deficient mice. The data presented included a sample size of n= 8 mice per group. *p< 0.05, **p< 0.01, and ***p<0.001 vs WT using one tailed student's t-test.

Furthermore, H&E staining showed more cellular infiltration around the eggs of *S. mansoni* parasites in the gut of *S. mansoni*-infected BATF2 deficient mice when compared to infected littermate controls (Figure 25).

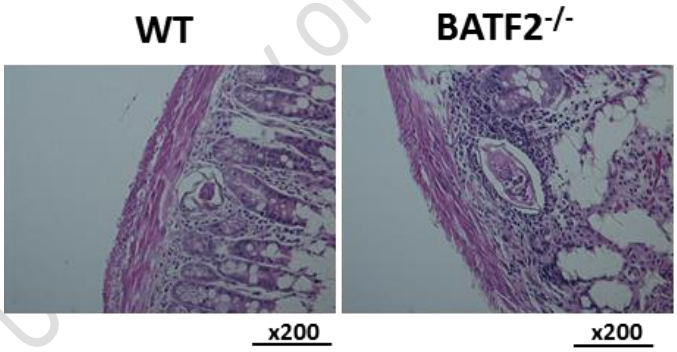

Figure 25. Increased cellular infiltration around *S. mansoni* eggs in BATF2 deficient mice. Representative H&E staining of gut sections for morphological analysis of the tissue.

Finally, fibrosis was assessed in the gut of *S. mansoni*-infected BATF2 deficient mice when compared to infected littermate controls (Figure 26). A representative CAB staining shows an increased fibrosis around the area surrounding the *S. mansoni* eggs (Figure 26A), and this was confirmed by hydroxyproline levels in the tissue, which were considerably elevated in the gut of *S. mansoni*-infected BATF2 deficient mice when compared to infected littermate controls (Figure 26B).

Taken together, our data indicates a heightened fibrogranulomatous inflammation and ensuing elevated fibrosis in the gut, but not the liver, of BATF2 deficient mice during schistosomiasis.

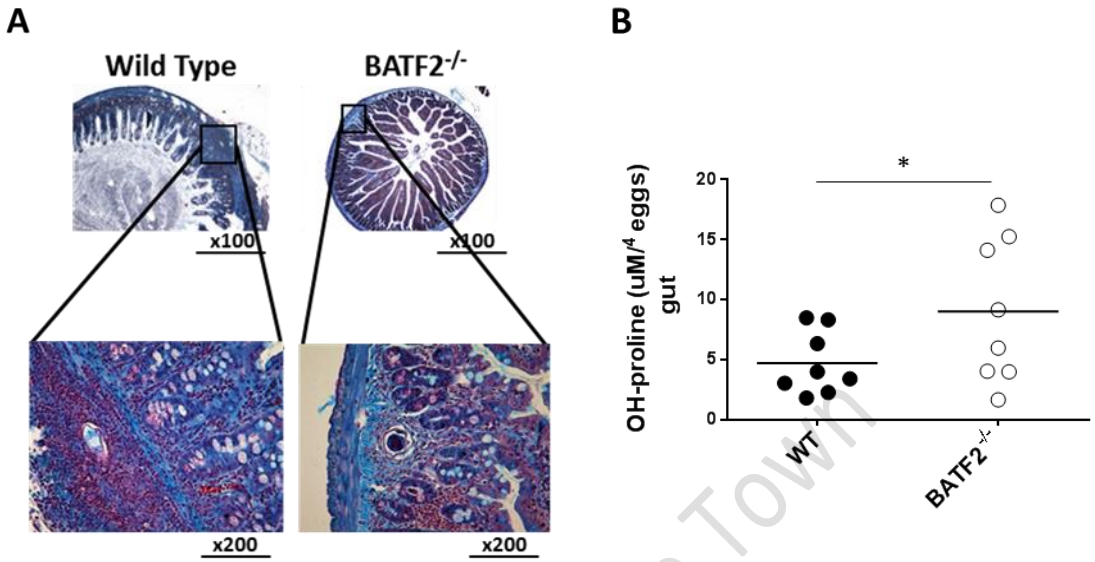

Figure 26. Increased fibrosis in BATF2 deficient mice during acute schistosomiasis. Representative CAB staining (A) for analysis of collagen content, and quantification of hydroxyproline levels (B) normalised to egg number to measure gut fibrosis. The data presented included a sample size of n= 8 mice per group. *p< 0.05, **p< 0.01, and ***p<0.001 vs WT using one tailed student's t-test.

3.5. BATF2 deficiency results in increased susceptibility of *S. mansoni*-infected mice during experimental acute schistosomiasis.

With reduced immunopathology in the liver and increased immunopathology in the intestine, we then aimed to further understand how this would affect the susceptibility of *S. mansoni*-infected BATF2 deficient mice when compared to infected littermate controls. To address this, both the wild type and BATF2 deficient mice were infected percutaneously with a dose of 80 live *S. mansoni* cercariae and monitored until the attainment of an ethically defined humane endpoint (persistent bloody diarrhoea, severe lethargy, weight loss of 20% or more). We noted that BATF2 deficient mice began to rapidly and prematurely drop in weight from week 8 post infection (Figure 27A). This rapid weight loss was accompanied by severe lethargy resulting in extensive premature mortality of *S. mansoni*-infected BATF2 deficient mice that all succumbed 12 weeks post infection leaving more than 50% of surviving *S. mansoni*-infected littermate controls (Figure 27B). Therefore, BATF2 deficiency renders mice considerably more susceptible to *S. mansoni* infection indicating a protective role for this transcription factor in the host survival during schistosomiasis, thus the initially reported expression of this factor as a result of schistosomiasis infection.

`

A

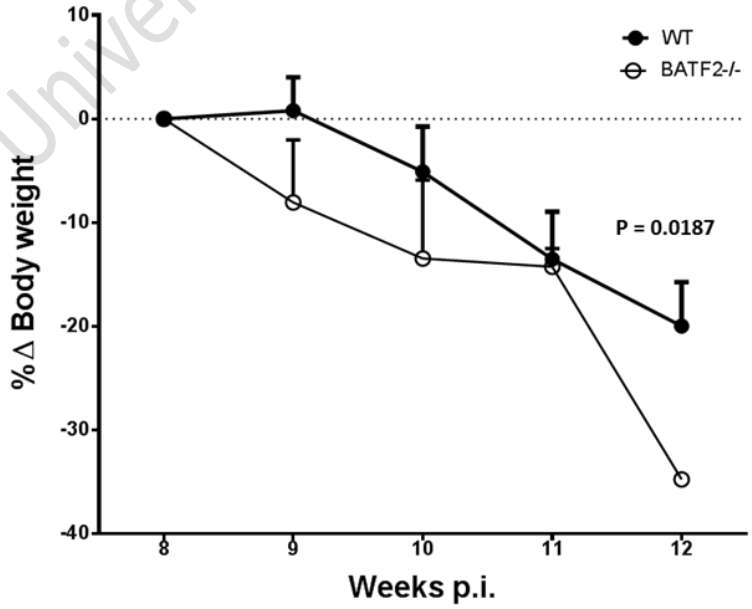

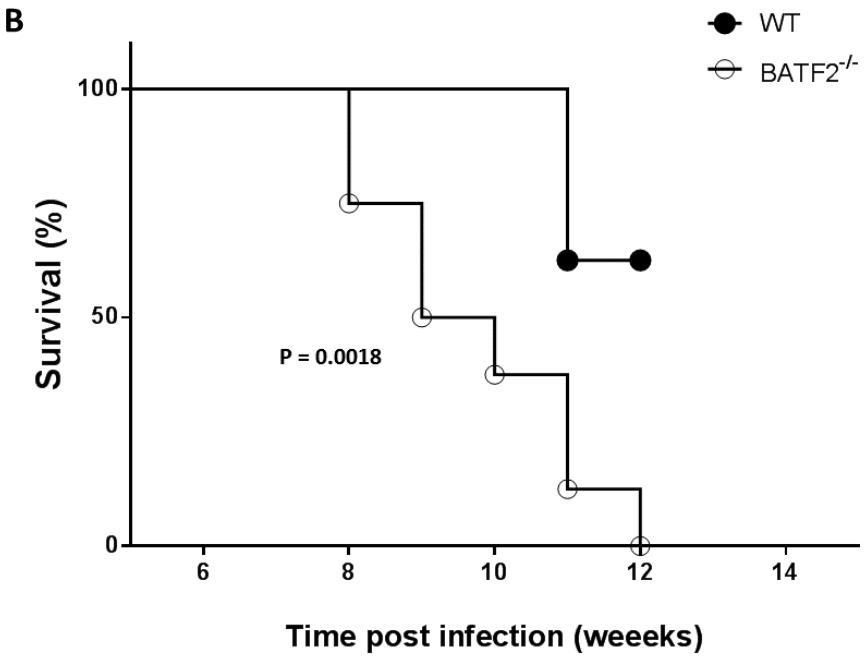

Figure 27. BATF2 is required for survival during *S. mansoni* infection. (A) Body weight change was measured weekly during the onset of infection. (B) Survival curve of Wild type (WT) and BATF2$^{-/-}$ mice. The data presented included a sample size of n= 8 - 10 mice per group. *p< 0.05, **p< 0.01, and ***p<0.001 vs WT using one tailed Chi square (Gehan-Breslow Wilcoxon test), and two-tailed student's *t*-test.

4. Discussion, conclusion and future work

Schistosomiasis is one of the tropically neglected diseases with the potential to cause morbidity and mortality in infected populations unless well controlled. Individuals or mice infected with *S. mansoni* usually develop liver and intestinal associated pathology that is characterised by the development of protective granulomas around the eggs lodged in the tissues and ultimately results in extensive egg-induced fibrosis. Both the granuloma formation and fibrosis are mediated by the host immune response during the infection, which include the moderate Th1 response to parasite antigens, and the dominant Th2 and Th17 responses to the egg-derived antigens (Wilson, 2007; Hams, 2013). Mechanisms which control the Th1, Th2, and Th17 cells are necessary to prevent severe tissue pathology (Wilson, 2007). In this study we propose a potentially important transcription factor called BATF2 which has the ability to control Th1, Th2, and Th17 linked fibrogranulomatous immunopathology in the intestine during experimental schistosomiasis.

Our work first confirmed the expression of BATF2 in liver and intestinal tissues at homeostasis and identified the potential effect of removing this transcription factor from the 129SvEv mice. Removal of the transcription factor did not affects most of the organs including the liver which showed no alteration in weight, tissue damage (ALT and AST levels), and or development of fibrosis in the tissue. This therefore, indicated that BATF2 expression might be dispensable to maintain liver homeostasis. However, in the case of the gut, a reduced length in the absence of BATF2 was observed pointing at a possible heightened inflammation in the gut of BATF2 deficient mice at homeostasis, consistent with reports linking reduced gut length and inflammation (Puapong 2006). In fact, we then noted an increase in pro-inflammatory type 1 (TNF-alpha), type 2 (IL-4, IL-5) and type 17 (IL-17) cytokine levels in the gut of BATF2 deficient mice at steady state. The effects of such an increased cytokine release were, however, not clinically relevant as no sign of pathology could be observed in BATF2 -deficient mice at homeostasis. In fact, despite the altered cellular distribution in several organs, clinical indicators of pathological inflammation such as serum cytokine IgE, liver

enzyme and cytokine levels as well as tissue fibrosis levels remained unchanged in BATF2 deficient mice at homeostasis. The observation of such subtle, albeit clinically inconsequent, changes observed in BATF2 deficient mice at homeostasis suggest a hitherto superficially understood role for this transcription factor in the gut homeostasis, particularly. Further experiments are clearly needed at this stage to address such subtleties. A possible way forwards could be the observation of inflammation control in the gut of aging BATF2 mice. More insights on the clear but so far clinically unapparent role of BATF2 in regulating pathology at homeostasis as per our present findings, should benefit from such an experiment. Several model of aging mice, have been used to unveil the role of host factors that reveal no clinical relevance in young mice at homeostasis (Wohlfert *et al.,* 2011; Rudra *et al.,* 2012), given the pervasive feature of aging tissues to display enhanced inflammation.

In this work, inflammation was brought in the form of schistosomiasis infection. In this setting, we first noted that BATF2 expression in the liver and the intestinal tissue was not reduced in response to acute schistosomiasis. Interestingly, the expression of BATF2 was elevated in the liver while in the intestine, it was maintained. This is rather intriguing, given the overall tendency of host factors to be considerably downregulated in the liver and gut tissues during murine schistosomiasis (Harvie, 2007; Manivannan, 2010). The fact that BATF2 escapes such a pattern of downregulation and has a maintained/increased tissue expression following *S. mansoni* infection further argues for a critical role of this factor during the disease. Possible avenues for explanation of such a need would be that i) BATF2 is a parasite-driven host factor meant to aid the parasite establishment in the host. Our own observation of a similar egg burden, thus parasite fitness in the livers and guts of *S. mansoni*-infected BATF2 deficient mice when compared to infected littermate controls strongly argues against this hypothesis. One could therefore rather consider that ii) the host expresses this factor in order to limit tissue pathology during schistosomiasis and preserve tissue integrity for survival.

In fact, we noted that BATF2 deficiency led to a massive expansion/recruitment of CD8+ dendritic cells and T-cells in the gut but not the liver of *S. mansoni*-

infected BATF2 deficient mice when compared to infected littermate controls supporting a negative regulatory role of BATF2 in gut inflammation during schistosomiasis. Strikingly, the pro-fibrotic nature of the cytokines abundantly released by gut T-cells in *S. mansoni*-infected BATF2 deficient mice when compared to infected littermate controls supports the role suggested for BATF2 in gut homeostasis in naïve mice. Importantly, given the pathological nature of schistosomiasis on the host gut, the consequences of BATF2 deficiency observed in naïve mice were exponentially worsened leading to aggravated gut fibrosis and granulomatous inflammation. Although it may seem confounding to have aggravated gut fibrosis in the presence of increased anti-fibrotic cytokine (IFNγ), the high ratio of IL-13 to IFNγ shown in figure 8, stands to reason for the observed pathology as previously demonstrated (Chiaramonte, 2003). It is therefore tempting and stands to reason to conclude here, overall, that BATF2 is critical for gut homeostasis even in naïve mice and in so doing constitutes a critical actor in the host ability to mitigate untoward gut fibrogranulomatous inflammation and pathological fibrosis during schistosomiasis. In fact, the premature wasting disease observed during schistosomiasis and the ensuing premature death in BATF2 deficient mice is quite indicative of uncontrolled gut pathology. In as much as we did not note gut bleeding as reported for other susceptible murine models (Herbert, 2004), the severe wasting disease suggests a compromised ability of the animals to feed thus possible enteropathy.

It is quite interesting that the frequencies of CD8+ dendritic cells were elevated in the gut of *S. mansoni*-infected BATF2 deficient mice when compared to infected littermate controls and that this most likely mediate the observed increase of Gut T cells observed. It could prove informative at this point to see if CD8 blockade would rescue the observed physical degradation in *S. mansoni*-infected BATF2 deficient mice when compared to infected littermate controls. Experiments aiming at addressing this point are currently underway and should shed more mechanistic insights on what the underlying bases of the susceptibility of *S. mansoni*-infected BATF2 deficient mice when compared to infected littermate controls are / might be. Moreover, the intestinal nature of the reported exacerbated pathology in *S. mansoni*-infected BATF2 deficient mice when compared to infected littermate controls begs the question of the role of the host

microbiome in the observed susceptibility of BATF2 deficient mice during schistosomiasis. Further tests on the animal gut microbial profile before and after schistosomiasis are also currently underway. With regard to the latter, co-housing experiments between *S. mansoni*-infected BATF2 deficient mice and *S. mansoni*-infected littermate controls have also been set. Whether BATF2 deficiency alter the gut fitness in a microbiome-dependent or independent manner should be uncovered by these experiments. As of yet, however, our findings clearly and unambiguously indicate that BATF2 deficiency compromises the host ability to control gut pathology and this is fatally exacerbated during schistosomiasis.

A rather puzzling observation in our work was the absence of heightened liver pathology in *S. mansoni*-infected BATF2 deficient mice when compared to infected littermate controls. In fact, the upregulation of BATF2 expression in the liver, rather than the sustained expression in the gut, would have suggested a more deleterious effect of BATF2 deficiency on the liver when compared to the gut. We noted, however, an amelioration of the hepatic parameters of *S. mansoni*-infected BATF2 deficient mice when compared to infected littermate controls i.e. reduced serum liver enzymes, reduced frequencies of liver T cells and reduced levels of liver fibrosis amid a maintained granulomatous response. This most likely defines a tissue-specific modus operandi for BATF2 where the expression in the liver promotes liver fibrosis and the expression in the gut refrain liver fibrosis. This theory of an organ specific and contradictory role for BATF2 during experimental schistosomiasis is further supported by our cellular and cytokinic profile in *S. mansoni*-infected BATF2 deficient mice when compared to infected littermate controls. In fact, whereas frequencies of CD8+ DCs are increased in the gut of *S. mansoni*-infected BATF2 deficient mice when compared to infected littermate controls, their frequency in the liver of *S. mansoni*-infected BATF2 deficient mice when compared to infected littermate controls is reduced. This parallels a cascade of antagonisms between the gut and the liver (High T cells and fibrosis in Gut vs low T cells and fibrosis in liver). What processes regulate the context-dependent function of BATF2 cannot be addressed with our present data. A possible way forward in trying to answer such a question could be the use of cell-specific BATF2 deficient mice.

Another possible explanation for the dual roles observed for BATF2 might resides in the established mechanistic feature of the factor itself. In fact, BATF2 only functions with binding partner(s) (Roy, 2015; Murphy, 2013). Such binding partners might be tissue-dependent and as such provide a mechanistic explanation for the apparently opposing role of BATF2 in the liver and gut. Since BATF2 lacks the DNA binding motif and usually mediate its function by binding with other transcription factors that have the DNA binding motif, we believe the function of the BATF2 will depend on the type of transcription factor it forms heterodimer with (Murphy, 2013). Therefore, more studies will need to be carried out to identify BATF2 binding partners which could potentially explain the differences observed in the liver as well as the intestinal tissue. This would also set a proof of principle to test the role of BATF2 in other organs and upon different infectious states. These endeavours would greatly not only from cell-specific but also tissue-specific BATF2 deficient mice.

In conclusion, our data indicate an unprecedented tissue-specific expression and role for BATF2 in regulating tissue inflammation, and fibroproliferative inflammation in health and schistosomiasis disease whereby an overall host protective role is defined for BATF2 expression in countering the excessive expansion of CD8+ DCs, CD4+ and CD8+ T cells in the gut of schistosomiasis-diseased mice therefore minimizing fibrogranulomatous inflammation and the consequent gut fibroproliferative pathology, morbidity and ultimately preventing mortality.

References:

Ahmed A.S. 2017. Schistosomiasis (Bilhazia). Treatment & Management. *MedScape*. Obtained on 05/08/2017. Website: http://emedicine.medscape.com/article/228392-treatment?src=refgatesrc1.

Banchereau J., Steinman R.M. 1998. Review: Dendritic cells and the control of immunity. *Nature*. **392**(6673):245-52.

Bao K., Carr T., Wu J., Bareclay W., Jin J., Ciofani M., Reinhardt L. 2016. BATF modulates the Th2 local control region and regulates CD4+ T cell fate during anthelminthic immunity. *Journal of Immunology.* ISSN: 1550-6606.

Barren L., Wynn T. A. 2011. Macrophage activation governs schistosomiasis-induced inflammation and fibrosis. *European Journal of Immunology*. **41**: 2509 – 2514.

Betz B.C., Jordan-Williams K.L., Wang C., Kang S.G., Liao J., Logan M.R., Kim C.H., Taparowsky E.J. 2010. Batf coordinates multiple aspects of B and T cell function required for normal antibody responses. *Journal of Experimental Medicine*. **207**: 933-942.

Bogen S.A., Flores Villanueva P.O., McCusker M.E., Fogelman I., el-Attar E.S., Kwan P., Stadecker M.J. 1995. In situ analysis of cytokine responses in experimental murine schistosomiasis. *Laboratory Investigation*. **73**: 252 – 258.

Boros D.V., Whitfield J.R., 1999. Enhanced Th1 and dampened Th2 responses synergises to inhibit Acute Granulomatous and Fibrotic responses in murine *schistosomiasis mansoni*. *Infections and Immunology*. **67:** 1187 – 1193.

Caffrey C.R. 2007. Chemotherapy of schistosomiasis: present and future. *Current opinion in chemical biology*. **11**: 433-9. doi:10.1016/j.cbpa.2007.05.031.

Cavalcanti M.G., de Araujo-Neto J.M., Peralta J.M. 2015. Schistosomiasis: Clinical management of liver disease. *Clinical Liver Disease*. **6**: 3.

Centers for Disease Control and Prevention. 2012. Parasite – Schistosomiasis. Obtained on 30/05/2017. Website : https://www.cdc.gov/parasites/schistosomiasis/biology.html

Chiaramonte M.G., Mentink-Kane M., Jacobson B.A., Cheever A.W., Whitters M.J., Goad M.E.P., Wong A., Collins M., Donaldson D.D., Grusby M.J., Wynn T.W. 2003. Regulation and Function of the Interleukin 13 Receptor α 2 During a T Helper Cell Type 2–dominant Immune Response. *Journal of Experimental immunology*. **197**: 687 – 701.

Chitsulo L., Engels D., Montresor A., Savioli L. 2000. The global status of schistosomiasis and its control. *Acta tropica*. **77**: 41-51.

de Jesus A.R., Silva A., Santana L.B., Magalhães A., de Jesus A.A., de Almeida R.P., Rêgo M.A.V., Burattini M.N., Pearce E.J., Carvalho E.M.. 2002. Clinical and immunologic evaluation of 31 patients with acute *schistosomiasis mansoni*. *Journal of Infectious Diseases.* **185**: 98–105.

Drugbank. 2013. Drugs: Praziquante. Obtained on 23/05/2016. Website: http://www.drugbank.ca/drugs/DB01058.

Dunne W.D., Cooke A. 2005. A Worm's Eye View of the Immune System: Consequences for Evolution of Human Autoimmune Disease. *Nature Reviews. Immunology*. **5**: 420 - 436.

Everts B., Tussiwand R., Dreesen L., Fairfax K.C., Huang S.C., Smith A.M, O'Neill C.M., Lam W.Y., Edelson B.T., Urban Jr. J.F., Murphy K.M., and Pearce E.J., 2016. Migratory CD103+ dendritic cells suppress helminth-driven type 2 immunity through constitutive expression of IL-12. *Journal of Experimental Medicine*. **213**: 35 – 51.

Fallon G.F., Mangan N.E., Suppression of Th2-type allergic reactions by helminth infection. *Nature reviews: Immunology.* **7**: 220 – 230.

Fonseca C.T., Oliveira S.C., Alves C.C., 2015. Eliminating schistosomes through vaccination: what are the best immune weapons?. *Frontiers in Immunology*. **6**: 1 – 8.

Gehman M.A., 2015. The role of BATF2 in LPS/IFNγ polarized macrophages. *Theses and Dissertations – Microbiology, Molecular Geneteics.* **10**.

Gryseels B., Polman K., Clerinx J., Kestens L. 2006. Human Schistosomiasis. *Lancet*. **368**: 1106 – 18.

Guler R., Roy S., Suzuki H., and Brombacher F. 2015. Targeting Batf2 for infectious diseases and cancer. *Oncotarget*. **6**: 26575 - 265829.

Haas W., Schmitt R. 1982. Characterisation of chemical stimuli for the penetration of *Schistosoma mansoni* cercariae. *Zeitschrift fu¨r Parasitenkunde.* **66**: 293–307.

Hammerich L., Heymann F., Tacke F. 2010. Role of IL-17 and Th17 cells in liver disease. *Clinical and Developmental Immunology.* **2011**: doi:10.1155/2011/345803.

Hams E., Aviello G., and Fallon P.G. 2013. The Schistosoma granuloma: Friend or foe? *Fronties in Immunology*. **4**: 89.

Harvie M., Jordan T.W., La Flamme A.C. 2007. Differential Liver Protein Expression during Schistosomiasis. *Infection and Immunology*. **75**: 736 – 744.

Herbert D.R., Hölscher C., Mohrs M., Arendse B., Schwegmann A., Radwanska M., Leeto M., Kirsch R., Hall P., Mossmann H., Claussen B., Förster I., Brombacher F. 2004. Alternative macrophage activation is essential for survival during schistosomiasis and downmodulates T helper 1 responses and immunopathology. *Immunity*. **20**: 623 – 635.

Hildner K., Edelson B. T., Purtha W. E., Diamond M., Matsushita H., Kohyama M., Calderon B., Schraml B.U., Unanue E.R., Diamond M.S., Schreiber R.D., Murphy T.L., and Murphy K.M., 2008. Batf3 deficiency reveals a critical role for CD8alpha+ dendritic cells in cytotoxic T cell immunity. *Science*. **322**: 1097-1100.

Hoffmann K.F., Cheever, A.W., Wynn, T.A. 2000. IL-10 and the dangers of immune polarization: Excessive type 1 and type 2 cytokine responses induce distinct forms of lethal immunopathology in murine shistosomiasis. *Journal of Immunology.* **164**: 6406 – 6416.

Hossain M., Norazmi M.N. 2013. Pattern Recognition Receptors and Cytokines in *Mycobacterium tuberculosis* Infection—The Double-Edged Sword? *BioMed Research International*. **2013**: 179174.

Hotez P.J., Molyneux D.H., Fenwick A., Ottesen E., Ehrlich Sachs, S., Sachs, J.D. 2006. Incorporating a rapid-impact package for neglected tropical diseases with programs for HIV/AIDS, tuberculosis, and malaria. *PLoS Medicine*. **3**: e102.

Ise W., Kohyama M., Schraml B.U., Zhang T., Schwer B., Basu U., Alt F.W., Tang J., Oltz E.M., Murphy T.L., Murphy K.M. 2011. The transcription factor BATF controls the global regulators of class-switch recombination in both B cells and T cells. *Nature Immunology*. **12**: 536-543.

Ismail M., Botros S., Metwally A., William S., Farghally A., Tao L.F., Day T.A., Bennett J.L. 1999. Resistance to praziquantel: direct evidence from *Schistosoma mansoni* isolated from Egyptian villagers. *American Society of Tropical Medicine and Hygiene*. **60**: 932 – 935.

King C.H. 2011. Schistosomiasis: Challenges and Opportunities. In: Institute of Medicine (US) Forum on Microbial Threats. The Causes and Impacts of Neglected Tropical and Zoonotic Diseases: Opportunities for Integrated Intervention Strategies. Washington (DC): National Academies Press (US); A12.

Kitada S., Kayama H., Okuzaki D., Koga R., Kobayashi M., Arima Y., Kumanogoh A., Murakami M., Ikawa M., Takeda K. 2017. BATF2 inhibits immunopathological Th17 responses by suppressing Il23a expression during Trypanosoma cruzi infection. *The Journal of Experimental Medicine*. https://doi.org/10.1084/jem.20161076.

Leeto M., Herbert D.R., Marillier R., Schwegmann A., Fick L., Brombacher F. 2006. TH1-dominant granulomatous pathology does not inhibit fibrosis or cause lethality during murine schistosomiasis. *The American Journal of Pathology*. **169**: 1701 – 1712.

Leshem E., Maor Y., Meltzer E., Assous M., Schwartz E. 2008. Acute Schistosomiasis Outbreak: Clinical Features and Economic Impact. *Clinical Infectious Diseases*. **47**: 1499.

Liu Z., Wei P.,Yang Y., Cui W., Cao B., Tan C., Yu B., Bi R., Xia K., Chen W., Wang Y., Zhang Y., Du X., and Zhou X., 2015. BATF2 deficiency promotes progression in human colorectal cancer via activation of HGF/MET signalling: A potential rationale for combining MET inhibitors with IFNs. *Clinical Cancer Research*. **21**: 1752 – 1763.

Loke P., Nair M.G., Parkinson J., Guiliano D., Blaxter M., Allen J.E. 2002. IL-4 dependent alternatively-activated macrophages have a distinctive in vivo gene expression phenotype. *BioMed Central immunology*, **3**: 7.

Ma H., Liang X., Chen Y., Pan K., Sun J., Wang H., Wang O., Li Y., Zhao J., Li J., Chen M., and Xia J., 2011. Decreased expression of BATF2 is associated with a poor prognosis in hepatocellular carcinoma. *International Journal of Cancer.* **128**: 771–777.

Ma H., Liang X., Chen Y., Pan K., Sun J., Wang H., Wang O., Li Y., Zhao J., Li J., Chen M., and Xia J., 2011. Decreased expression of BATF2 is associated with a poor prognosis in hepatocellular carcinoma. *International Journal of Cancer.* **128**: 771–777.

Manivannan B., Rawson P., Jordan T.W., Secor W.E., La Flamme A.C. 2010. Differential Patterns of Liver Proteins in Experimental Murine Hepatosplenic Schistosomiasis. *Infection and Immunology*. **78**: 618 – 628.

Mart´ınez-L´opez M., Iborra S., Conde-Garrosa R., Sancho D. 2015. Batf3-dependent CD103+ dendritic cells are major producers of IL-12 that drive local Th1 immunity against Leishmania major infection in mice. *European Journal of Immunology*. **45**: 119 – 129.

Mayer J.U., Demiri M., Agace W.W., MacDonald A.S., Svensson-Frej M., Milling S.W. 2017. Different populations of CD11b+ dendritic cells drive Th2 responses in the small intestine and colon. *Nature Communications*. **8**: 15820.

Medzhitov R. 2007. Recognition of microorganisms and activation of the immune response. *Nature*. **449**: 819 – 826.

Melman S.D., Steinauer M.L., Cunningham C., Kubatko L.S., Mwangi I.N., Wynn N.B., Mutuku M.W., Karanja D.M., Colley D.G., Black C.L., Secor W.E., Mkoji G.M., Loker E.S. 2009. Reduced Susceptibility to Praziquantel among Naturally Occurring Kenyan Isolates of *Schistosoma mansoni*. *PLoS Neglected Tropical Diseases*. **3**(8):e504. doi: 10.1371/journal.pntd.0000504.

Mentink-Kane M.M., Cheever A.W., Thompson R.W., Hari D.M., Kabatereine N.B., Vennervald B.J., Ouma J.H., Mwatha J.K., Jones F.M., Donaldson D.D., Grusby

M.J., Dunne D.W., Wynn T.A. 2004. IL-13 receptor alpha 2 down-modulates granulomatous inflammation and prolongs host survival in schistosomiasis. *Proceedings of the National Academy of Sciences.* **101**: 586 – 590.

Murphy T. L., Tussiwand R., and Murphy K. M., 2013. Specificity through cooperation: BATF–IRF interactions control immune-regulatory networks. *Nature review, Immunology.* **13:** 499.

Nono J.K., Ndlovu H. , AbdelAziz N., Mpotje T., Hlaka L., Brombacher F. Host regulation of liver fibroproliferative pathology during experimental schistosomiasis via interleukin-4 receptor alpha. *PLoS Neglected Tropical Diseases*. In press.

Oh J., Shin J.S. 2015. The role of dendritic cells in central tolerance. *Immune network*. **15**(3): 111 – 120.

Olds G.R. 2003. Administration of praziquantel to pregnant and lactating women. *Acta tropica*. **86**: 185 – 195.

O'Neill S.M., Brady M.T., Callanan J.J., Mulcahy G., Joyce P., Mills K.H., Dalton J.P. 2000. Fasciola hepatica infection downregulates Th1 responses in mice. *Parasite Immunol*ogy. **22:** 147-155

Pearce E.J. 2005. Priming of the immune response by schistosome eggs. *Parasite Immunology*. **27:** 265 – 270.

Pearce E.J., MacDonald A.S. 2002. The immunobiology of schistosomiasis. *Nature Review, Immunology.* **2:** 499.

Pedras-Vasconcelos J.A., and Pearce E.J. 1996. Type 1 CD8+ T cell responses during infection with the helminth *Schistosoma mansoni*. *Journal of Immunology*. **157**: 3046-3053.

Platt A. M. 2017. Immunity in the gut. British Society for Immunology. Obtained on 26 October 2017.

Puapong D.P., Wu B.M., Lam M.M., Atkinson J.B., Dunn J.C.Y. 2006. Distension enterogenesis: increasing the size and function of small intestine. *Journal of Pediatric Srugery*. **41**: 763 – 767.

Ramadan M.E., Ramadan M.E.E., Mervat Shafik Mohamed Yousef M.S.M. 2013. Role of TNF alpha in *schistosoma mansoni* infection and cirrhotic liver. *International Journal of Pharmaceutical and Medical Research*. **1**: 6 – 12.

Ramalingam T.R., Gieseck R.L., Acciani T.H., Hart K.M., Cheever A.W., Mentink-Kane M.M., Vannella K.M., Wynn T.A. 2016. Enhanced protection from fibrosis and inflammation in the combined absence of IL-13 and IFN-γ. *Journal of Pathology*. **239**: 344 – 354.

Rivera J., Tessarollo L. 2008. Genetic Background and the Dilemma of Translating Mouse Studies to Humans. *Immunity*. **28**: 1 – 4.

Romagnani S. 1992. Induction of Th1 and Th2 responses: a key role for the 'natural' immune response?. *Immunology Today.* **13**: 379 – 381.

Ross A.G.P., Bartly P.B., Sleigh A.C., Olds G.R., Li Y., Williams G.M., McManus D.P. 2002. Schistosomiasis. *The new England Journal of Medicine*. **346**: 1212 – 1220.

Roy S., Guler R., Parihar S.P., Schmeier S., Kaczkowski B., Nishimura H., Shin J. W., Negishi Y., Ozturk M., Hurdayal R., Kubosaki A., Kimura Y., de Hoon M. J. L., Hayashizaki Y., Brombacher F., and Suzuki H. 2015. BATF2/Irf1 induces inflammatory responses in classically activated macrophaes, lipopolysacharides, and mycobacterial infection. *Journal of Immunology*. **194**: 6035-6044.

Rudra D., deRoos P., Chaudhry A., Niec R.E., Arvey A., Samstein R.M., Leslie C., Shaffer S.A., Goodlett D.R., Rudensky A.Y. 2012. Transcription factor Foxp3 and its protein partners form a complex regulatory network. *Nature Immunology*. **13**: 1010 – 1019.

Rutitzky L.I., Stadecker M.J. 2006. CD4 T cells producing pro-inflammatory interleukin-17 mediate high pathology in schistosomiasis. *Memórias do Instituto Oswaldo Cruz, Rio de Janeiro*. **101**: 327 – 330.

Sabin Vaccine Institute. 2015. Schistosomiasis. *Global Network: Neglected Tropical Disease*. Obtained on 30/05/2017: http://www.globalnetwork.org/schistosomiasis

Schmiedel Y., Mombo-Ngoma G., Labuda L.A., Janse J.J., de Gier B., Adegnika A.A., Issifou S,, Kremsner P.G., Smits H.H.,, Yazdanbakhsh M. 2015.

CD4+CD25hiFOXP3+ Regulatory T Cells and Cytokine Responses in Human Schistosomiasis before and after Treatment with Praziquantel. *PLoS Neglected Tropical Diseases*. **9**: e0003995. doi:10.1371/journal.

Sokolow S.H., Wood C.L., Jones I.J., Swartz S.J., Lopez M., Hsieh M.H., Lafferty K.D., Kuris A.M., Richards C., De Leo G.A. 2016. Global Assessment of Schistosomiasis Control Over the Past Century Shows Targeting the Snail Intermediate Host Works Best. *PLoS Neglected Tropical Diseases*. **10** (7): e0004794.

Sorini C., Falcone M. 2013. Shaping the (auto)immune in the gut: the role of intestinal immune regulation in the prevention of type 1 diabetes. *American Journal of Clinical and Experimental Immunology*. **2:** 156 – 171**.**

Tomasello E., Bedoui S. 2013. Intestinal innate immune cells in gut homeostasis and immunosurveillance. *Immunology and Cell Biology*. **91**: 201–203.

Tussiwand R., Lee W., Murphy T.L., Mashayekhi M., Wumesh K.C., Albring J.C., Satpathy A.T., Rotondo J.A., Edelson B.T., Kretzer N.M., Wu X., Weiss L.A., Glasmacher E, Li P., Liao W., Behnke W, Lam S.S. K., Aurthur C.T., Leonard W.J., Singh H., Stallings C.L., Sibley L.D., Schreiber R.D., Murphy K.M. 2012. Compensatory dendritic cell development mediated by BATF-IRF interactions. *Nature*. **490**: 502 – 507.

Vale N., Gouveia M.J., Rinaldi G., Brindley P.J., Gärtner F., Correia da Costa J.M.C. 2017. Praziquantel for schistosomiasis, single drug revisited metabolism, mode of action and resistance. *American Society for Microbiology*. doi:10.1128/AAC.02582-16.

Van Dam G.J., Wichers J.H., Falcao Ferreira T.M., Ghati D., van Amerongen A., Deelder A.M. 2004. Diagnosis of Schistosomiasis by Reagent Strip Test for Detection of Circulating Cathodic Antigen. *Journal of Clinical Microbiology*. **42**: 5458 – 5461.

van der Werf, M.J., de Vlas S.J., Brooker S., Looman C.W.N., Nagelkerke N.J.D., Habbema J.D.F., Engels D. 2003. Quantification of clinical morbidity associated with schistosome infection in sub-Saharan Africa. *Acta tropica*. **86**: 125-39.

Wang B., Liang S., Wang Y., Zhu X., Gong W., Zhang H., Li Y., Xia C. 2015. Th17 Down-regulation Is Involved in Reduced Progression of Schistosomiasis Fibrosis in ICOSL KO Mice. *PLoS Neglected Tropical Diseases*. **11**: e0003434. doi:10.1371/journal.pntd.0003434.

Weaver L.T., Austin S., Cole T.J. 1991. Small intestinal length: a factor essential for gut adaptation. *British Society of Gastroenterology*. **32**: 1321 – 1323.

Wen H., Chen Y., Hu Z., Mo Q., Tang J., and Sun C., 2014. Decreased expression of BATF2 is significantly associated with poor prognosis in oral tongue squamous cell carcinoma. *Oncology Reports*. **31**: 169 – 174.

Wilson M.S., Mentink-Kane M.M., Pesce J.T., Ramalingam T.R., Thompson R., Wynn T.A. 2007. Immunopathology of schistosomiasis. *Immunology and Cell Biology*. **85:** 148–154.

Wohlfert E.A., Grainger J.R., Bouladoux N., Konkel J.E., Oldenhove G., Ribeiro C.H., Hall J.A., Yagi R., Naik S., Bhairavabhotla R., Paul W.E., Bosselut R., Wei G., Zhao K., Oukka M., Zhu J., Belkaid Y. 2011. GATA3 controls Foxp3^{+} regulatory T cell fate during inflammation in mice. *The Journal of Clinical Investigation*. **121**: 4503 – 4515.

World Health Organisation. 2016. Schistosomiasis. Obtained on 23/05/2016. Website: http://www.who.int/mediacentre/factsheets/fs115/en/.

World Health Organization. 2017. Schistosomiasis: The disease. Obtained on 30/05/2017: http://www.who.int/schistosomiasis/disease/en/

Wynn T.A., Cheever A.W., Williams M.E., Hieny S., Caspar P., Kühn R., Müller W., Sher A. 1998. IL-10 regulates liver pathology in acute murine *schistosomiasis mansoni* but is not required for immune down modulation of chronic disease. *Journal of Immunology*. **160**: 4473 – 4480.

Wynn T.A., Eltoum I., Cheever A.W., Lewis F.A., Gause W.C., Sher A. 1993. Analysis of cytokine mRNA expression during primary granuloma formation induced by eggs of Schistosoma mansoni. *Journal of Immunology.* **153**: 1430 – 1440.

Yang Z., Chen Y., Lillo C., Chien J., Yu Z., Michaelides M., Klein M., Howes K. A., Li Y., Kaminoh Y., Chen H., Zhao C., Chen Y., Al-Sheikh Y. T., Karan G., Corbeil D.,

Escher P., Kamaya S., Li C., Johnson S., Frederick J. M., Zhao Y., Wang C., Cameron D. J., Huttner W. B., Schorderet D. F., Munier F. L., Moore A. T., Birch D. G., Baehr W., Hunt D. M., Williams D. S., and Zhang K. 2009. Th2 cell hyporesponsiveness during chronic murine schistosomiasis is cell intrinsic and linked to GRAIL expression. *The Journal of Clinical Investigation*. **119**: 1396.

Zhu J., Xu, Z., Chen, X., Zhou, S., Zhang, W., Chi, Y., Li, W., Song, X. 2014. Parasitic antigens alter macrophage polarization during *Schistosoma japonicum* in mice. *Parasites & Vectors*. **7**: 122.

Appendix 1

List of FACS antibodies used

Antibody	Conjugate	Type	Company	Catalogue number	Dilution used
CD3	A700	Hamster antyi-mouse	BD Biosciences	557984	1:160 of 0.2 mg/ml
CD4	FITC	Rat anti-mouse	BioLegend	100510	1:640 of 0.5mg/ml
CD8	V500	Rat anti-mouse	BD Biosciences	560776	1:320 of 0.2mg/ml
CD11b	V450	Rat anti-mouse	BD Biosciences	560455	1:640 of 0.2mg/ml
CD11c	A700	Hamster anti-mouse	BD Biosciences	560583	1:320 of 0.2mg/ml
F4/80	PE-cy7	Rat anti-mouse	Affymetrix eBioscience	25-4801-82	1:320 of 0.2mg/ml
Siglec-F	APC	Rat anti-mouse	BD Biosciences	562680	1:160 of 0.2mgml
Ly6G	APC-Cy7	Rat anti-mouse	Sony Biotechnology Inc	1238120	1:640 of 100µg/ml
CD45	PE	Rat anti-mouse	BD Biosciences	553081	1:320 of 0.2mgml
CD45	Biotin	Rat anti-mouse	BD Bioscience	553078	1:1280 of 0.5 mg/ml
7AAD	PerCP-Cy5.5		SIGMA	A9400	1:1000
Lin	PerCP-Cy5.5	Mouse	BD Bioscience	561317	1:50
ICOS	APC	Rat anti-mouse	BD Biosciences	563469	1:320 of 0.2mg/ml
T1ST2	FITC	Rat anti-mouse	MD Biosciences	101001F	1:640 of 0.5 mL
IL-4	PerCP-Cy5.5	Rat anti-mouse	BD Bioscience	560700	1:50 of 0.2mg/ml
IL-5	PE	Rat anti-Mouse/Human	BD Bioscience	554395	1:50 of 0.2mg/ml
IL-13	PE-Cy7	Rat anti-mouse	Affymetrix eBioscience	25-7133-82	1:50 of 0.2mg/ml
IL-17	APC-Cy7	Rat anti-mouse	BD Biosciences	560821	1:50 of 0.2mg/ml
Streptavidin	PerCP-Cy™5.5		BD Biosciences	551419	1:1000 Of 0.2mg/ml

Appendix 2

List of cytokine/proteins used for ELISA

Cytokine or antibody		Company	Catalogue number	Dilution used	Clone
IFN-gamma	Primary	Home-made (UCT)		1:500 Of 3.4782 mg/ml	AN18.KL6
	secondary	BD Biosciences	554410	1:1000 Of 0.5mg/ml	
	Standard	BD Biosciences	554587	200ng/ml	
TNF-alpha	Primary	BD Biosciences	551225	1:500 of 0.5mg/ml	
	secondary	PharMingen	1B122D	1:500 Of 0.5mg/ml	
	Standard	BD Bioscience	554589	200ng/ml	
TGF-beta	Primary	BD Biosciences	555052	1:250 Of 0.5mg/ml	A75-2
	secondary	BD Biosciences	555053	1:500 Of 0.5mg/ml	A75-3
	Standard	WhitSci	240-B-002	100ng/ml	
IL-1 alpha	Primary	BD Biosciences	550604	1:250 Of 0.5mg/ml	
	secondary	BD Biosciences	550606	1:500 Of 0.5mg/ml	
	Standard	WhitSci	400-ML-005	100ng/ml	
IL-4	Primary	Home-made (UCT)		1:500 Of 2.065mg/ml	11B11
	Secondary	BD Biosciences	554390	1:1000 Of 0.5mg/ml	
	Standard	BD Biosciences	550067	100ng/ml	
IL-5	Primary	BD Biosciences	554393	1:500 Of 0.5mg	
	secondary	BD Biosciences	554397	1:500 Of 0.5mg	
	Standard	BD Biosciences	554581	100ng/ml	
IL-6	Primary	BD Biosciences	554400	1:250 Of 0.5mg/ml	
	secondary	BD Biosciences	554402	1:500 Of 0.5mg/ml	
	Standard	BD Bioscience	554582	100ng/ml	
IL-10	Primary	WhitSci	MAB417-500	1:500 Of 500µg	JES052A5
	Secondary	Biocom Biotech	504906	1:1000	
	Standard	WhitSci	417-ML-005	100ng/ml	
IL-13	Primary	R&D systems	840249	1:500 Of 240µg/0.5mL	38213

	secondary	R&D systems	840250	1:500 Of 12µg/mL	
	Standard	R&D systems	840251	100ng/ml	
IL-17	Primary	Biolegend	506902	1/500 Of 500µg	
	secondary	Biolegend	507022	1/500 Of 50µg	
	Standard	WhitSci	421-ML-025	100ng/ml	